Stephanie Anna Gärtner

Characterization of *Aerococcus viridans* L-lactate oxidase Y215F and Y215H mutants

Masterarbeit

Zur Erlangung des akademischen Grades

einer Diplom-Ingenieurin

der Studienrichtung Biotechnologie

an der

Technischen Universität Graz

Univ.-Prof. Dipl.-Ing. Dr. techn. Bernd Nidetzky

Institut für Biotechnologie und Bioprozesstechnik

Technische Universität Graz

2011

If I have a thousand ideas and
only one turns out to be good,
I am satisfied.

(Alfred Bernhard)

Beschluss der Curricula-Kommission für Bachelor-, Master- und Diplomstudien vom 10.11.2008

Genehmigung des Senates am 1.12.2008

EIDESSTATTLICHE ERKLÄRUNG

Ich erkläre an Eides statt, dass ich die vorliegende Arbeit selbstständig verfasst, andere als die angegebenen Quellen/Hilfsmittel nicht benutzt, und die den benutzten Quellen wörtlich und inhaltlich entnommene Stellen als solche kenntlich gemacht habe.

Graz, am …… ……..

(Unterschrift)

STATUTORY DECLARATION

I declare that I have authored this thesis independently, that I have not used other than the declared sources / resources, and that I have explicitly marked all material which has been quoted either literally or by content from the used sources.

Graz,…… ……..

(signature)

Danksagung

Dank, wem Dank gebührt.

Abstract

L-lactate oxidase from *Aerococcus viridans* belongs to the family of L-α-hydroxy acid oxidizing enzymes and catalyses the conversion of L-lactate and oxygen to pyruvate and hydrogen peroxide. It is used in biosensors for the determination of L-lactate level in blood and food.

L-lactate oxidase is able to convert also other L-α-hydroxy acids, e.g. glycolic acid. This cross-reaction in biosensors for medical use can lead to false diagnoses. The aim of the present work was to improve the specificity for L-lactate by site-directed mutagenesis in the active site of L-lactate oxidase. Two mutants Y215F and Y215H were constructed and analyzed. Neither an increase of specific activity for L-lactate, nor a significant decrease of specific activity for glycolic acid for both of the mutants could be observed.

PH studies for the wild type and Y215F were conducted to find out more about the mechanism of the enzyme and the role of Tyr^{215}. Y215F showed a slightly lower pK_2 of about 7 compared to the wild type with a pK_2 of about 8. The presence of the pK_2 in the enzyme indicates that there is an active site residue (or a group of residues), which has to be protonated for optimum enzyme activity. As tyrosine has a pK of about 10, the mentioned residue might not be Tyr^{215}, but Tyr^{215} might influence the pK of the enzyme.

Based on the results of the present work, Tyr^{215} residue in L-lactate oxidase is an active site residue (Leiros et al. 2006) of big interest for further experiments and analyzes. Stopped-flow measurements are going to be performed in the near future to complement the results of the pH studies and to give more information about the influence of the pH on the reductive and oxidative half-reaction.

Zusammenfassung

L-Laktatoxidase aus *Aerococcus viridans* gehört zur Enzymfamilie der L-α-hydroxysäure-oxidierenden Enzyme und katalysiert die Reaktion von L-Laktat und Sauerstoff zu Pyruvat und Wasserstoffperoxid. Das Enzym findet Anwendung in Biosensoren zur quantitativen Bestimmung von L-Laktat in Blut und im Lebensmittelbereich.

L-Laktatoxidase reagiert nicht nur mit L-Laktat als Substrat, sondern auch mit anderen L-α-Hydroxysäuren, wie der Glykolsäure. Diese mögliche, parallele Reaktion kann in Biosensoren im medizinischen Bereich zu falschen Diagnosen führen. Das Ziel der vorliegenden Arbeit war es, die Spezifität der L-Lakatoxidase für L-Laktat mittels zielgerichteter Mutagenese an der active site zu verbessern. Es wurden dafür zwei Mutanten – Y215F und Y215H – konstruiert und analysiert. Kinetische Analysen zeigten weder eine Zunahme der spezifischen Aktivität für L-Laktat, noch eine signifikante Abnahme der spezifischen Aktivität gegenüber Glykolsäure für beide Mutanten.

Desweiteren wurden pH-Studien für den Wildtyp und Y215F durchgeführt, um den genauen Mechanismus des Enzyms und die Funktion von Tyr^{215} erklären zu können. In Y215F war der pK_2 des Enzyms mit ungefähr 7 etwas niedriger als der des Wildtyps mit einem pK_2 von ungefähr 8. Die pH-Studien zeigten, dass ein active site-Aminosäurerest oder eine Gruppe an Aminosäuren protoniert vorliegen muss, um optimale Enzymaktivität zu gewährleisten. Da Tyrosin einen pK von ungefähr 10 hat, ist dieser Rest vermutlich nicht Tyr^{215}. Tyr^{215} könnte jedoch den pK des Enzyms beeinflussen.

Die Ergebnisse der folgenden Arbeit bestätigen das große Interesse an dem active site-Aminosäurerest Tyr^{215} (Leiros et al. 2006) und geben Anlass zu weiteren Experimenten und Analysen. In naher Zukunft werden stopped-flow-Messungen durchgeführt. Diese sollen die Ergebnisse der pH-Studien ergänzen und genauere Informationen über den Einfluss des pH-Werts auf die reduktive und oxidative Halbreaktion geben.

Table of Contents

1. Introduction

L-lactate oxidase (LOX) from *Aerococcus viridans* catalyzes the conversion of L-lactate and oxygen to pyruvate and hydrogen peroxide. It is a well-studied enzyme as far as biochemical characterizations as well as the determination of the crystal structure under various conditions are concerned (Maeda-Yorita et al. 1995, Leiros et al. 2006).

Among other applications, L-lactate oxidase is mainly used in biosensors for the determination of L-lactate levels in medical and food analytics. These biosensors potentiometrically detect hydrogen peroxide. Multianalytic sensors for the simultaneous determination of glucose (with glucose oxidase as enzyme), uric acid (uricase as oxidase) and L-lactate have also been developed for clinical diagnostics (Frebel et al. 1997). The biosensor reactions occur in solution as well as via gas analytics (Leiros et al. 2006, Pernet et al. 2009). In literature some inconveniences according to the LOX used in biosensors are published. On the one hand LOX is often not stable enough under conditions used in biosensors. On the other hand LOX does react not only with L-lactate as substrate, but also with other L-α-hydroxy acids (Leiros et al. 2006).

One cross-reaction of L-lactate oxidase with an alternative substrate, which is of particular interest in medical science, is the oxidation of glycolic acid. Glycolic acid is generated during the primary metabolism of ethylene glycol in the liver by ADH. The ingestion of ethylene glycol leads to ethylene glycol poisoning, which is a medical emergency. A reaction of glycolic acid with L-lactate oxidase in blood gas analyzers may induce false elevation of blood lactate and therefore a false diagnosis and medical treatment (Pernet et al. 2009).

The aim of the present work was to change substrate specificity of L-lactate oxidase and to find out more about the mechanism of the LOX by site-directed mutagenesis of an active site amino acid residue.

1.1. L-lactate oxidase - an FMN-dependent α-hydroxy acid oxidizing enzyme

L-lactate oxidase from *Aerococcus viridans* is a tetramer with a size of 164 kDa. FMN functions as cofactor in the reaction of L-lactate conversion (Maeda-Yorita et al. 1995, Leiros et al. 2006). (See Figure 1-1).

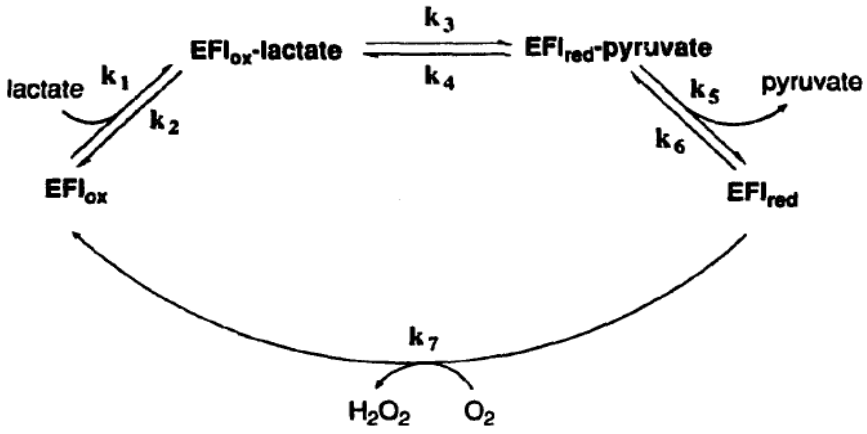

Figure 1-1 **Reaction pathway of L-lactate oxidase (Maeda-Yorita et al. 1995)**

Other members of the family of L-α-hydroxy acid oxidizing flavoproteins are L-lactate monooxygenase, flavocytochrome b_2, glycolate oxidase, mandelate dehydrogenase and a long chain α-hydroxy-acid oxidase (Maeda-Yorita et al. 1995, Leiros et al. 2006).

Remarkable similarities in properties of these enzymes result among others from a similarity in structure. L-α-hydroxy acid oxidizing enzymes possess six conserved amino acids in the active site. There is only one exception: in long chain α-hydroxy acid oxidase there is a phenylalanine residue found instead of tyrosine (Tyr^{40} in LOX) (Maeda-Yorita et al. 1995, Fitzpatrick et al. 2001). The active site of the flavoenzymes with its conserved amino acid residues and their postulated functions is illustrated in Figure 1-2.

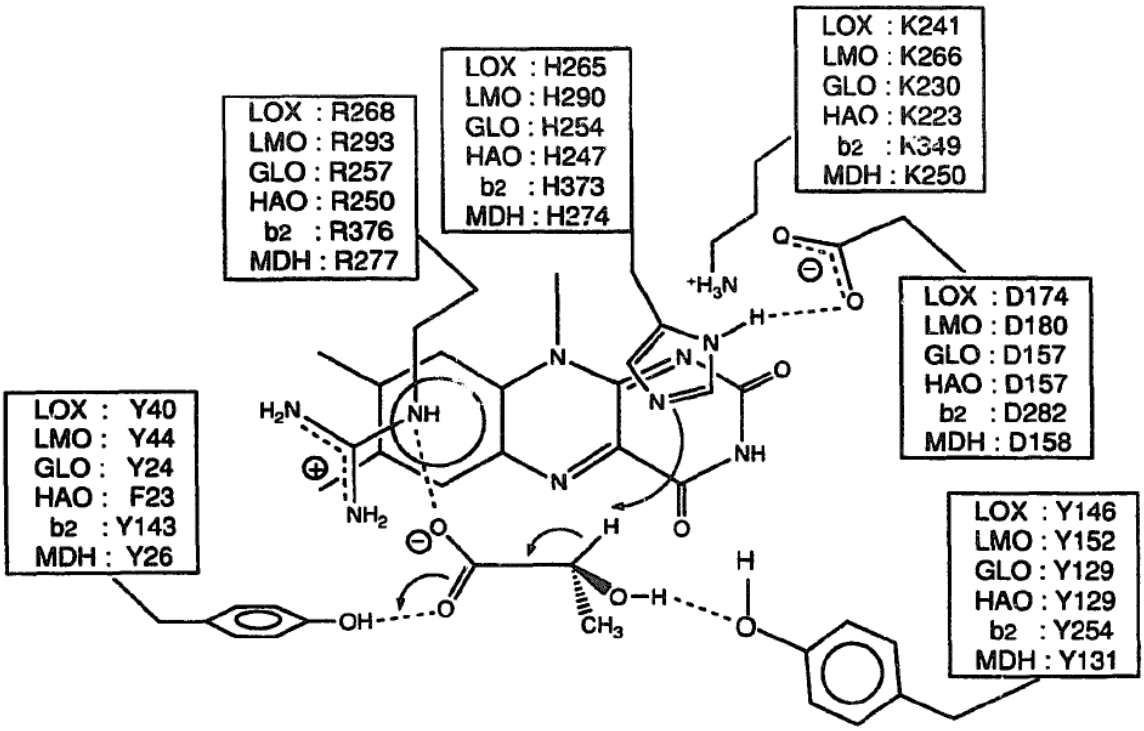

Figure 1-2 **Conserved amino acid residues and their functions in L-α-hydroxy acid oxidizing flavoproteins (Maeda-Yorita et al. 1995)**

Maeda-Yorita et al. (1995) reported the role of every single conserved amino acid. The tyrosine close to the carboxyl group (Tyr^{40} in LOX) and the arginine (Arg^{268} in LOX) residues are probably involved in substrate binding. The histidine (His^{265} in LOX) residue is postulated to abstract a proton of the substrate - even the α-proton or the hydroxyl proton (see Figure 1-3) - and lysine (Lys^{241} in LOX) to stabilize the anionic form of the FMN. Aspartate (Asp^{174} in LOX) probably stabilizes the protonated histidine. Of particular interest is the tyrosine (Tyr^{146} in LOX) residue which interacts with the hydroxyl group of the substrate (Maeda-Yorita et al. 1995).

The reaction is split in two half-reactions – the reductive followed by the oxidative. First the L-α-hydroxy acid substrate is oxidized by the enzyme and an α-keto acid is formed as first product. In this step FMN is reduced to hydroquinone. The re-oxidation of FMN occurs during the oxidative half-reaction by oxygen as electron acceptor. It seems as if only the oxidative half-reaction differs among the members of the enzyme family (Maeda-Yorita et al. 1995, Furuichi et al. 2008, Leiros et al. 2006).

For the reductive half-reaction there are two possible reaction mechanisms discussed. One mechanism leads to the formation of a carbanion intermediate by the deprotonation of the α-carbon

of the substrate by a catalytic histidine (His^{265} in LOX) and subsequent reduction of FMN. For the hydride transfer mechanism the catalytic base (His^{265} in LOX) abstracts the proton of the hydroxyl group and the α-carbon hydrogen is transferred to FMN, which leads to the reduction of the FMN (Sobrado et al. 2003, Furuichi et al. 2008). (See Figure 1-3)

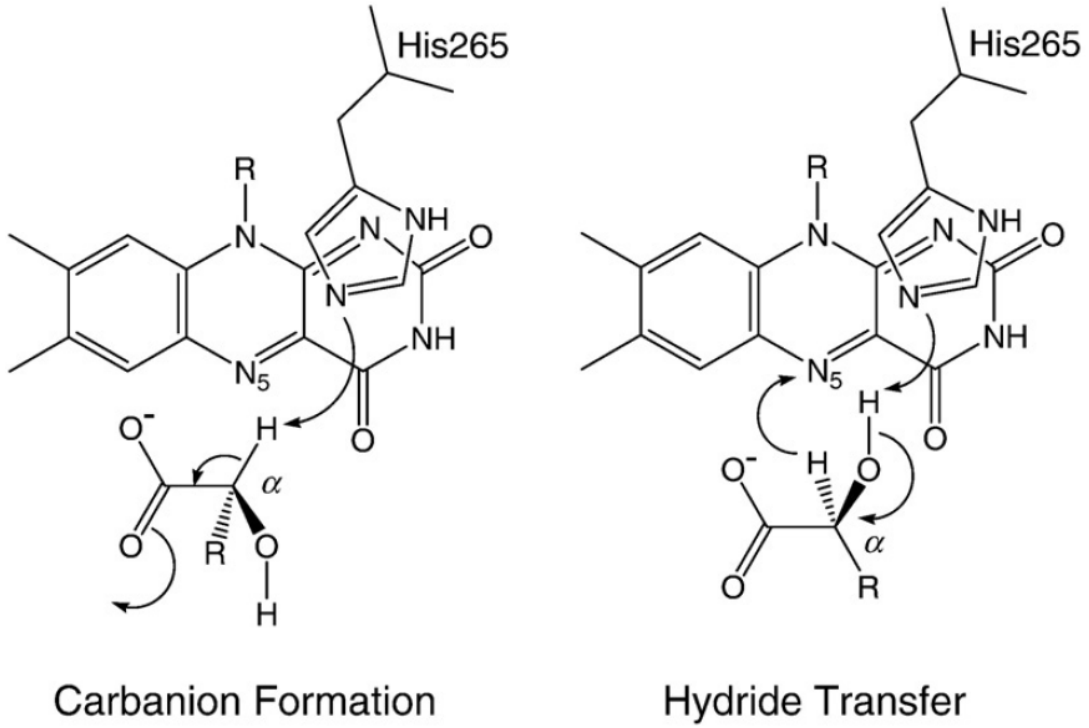

Figure 1-3 **Possible mechanisms of the reductive half-reaction in L-α-hydroxy acid oxidizing enzymes, demonstrated for L-lactate oxidase (Furuichi et al. 2008)**

1.2.Site-directed mutagenesis at Tyr^{215} in L-lactate oxidase

Besides Tyr^{146} there is another tyrosine residue in L-lactate oxidase close to the substrate of particular interest, namely Tyr^{215}. This residue is not conserved within the L-α-hydroxy acid oxidizing flavoproteins. The hydroxyl group of Tyr^{146} is close to the hydroxyl group of L-lactate (2.62 Å), as well as Tyr^{215} (2.56 Å). Because of the proximity to the hydroxyl group of the substrate Tyr^{215} could be involved in substrate stabilization (Leiros et al. 2006). Thus site-directed mutagenesis at Tyr^{215} could give more information about the role of this active site residue. Furthermore it could influence the substrate specificity of the enzyme (Maeda-Yorita et al. 1995, Sobrado et al. 2003).

Thus, two mutants were constructed: tyrosine was replaced by the nonpolar residue phenylalanine, which lacks the hydroxyl group for hydrogen bond interaction with the substrate, and by histidine, which could provide an alternative hydrogen bond and could stabilize the anionic form of the substrate. In addition, mutations change the pK of the residue, which could have an influence on the entire reaction mechanism.

In Figure 1-4 the active site of L-lactase oxidase with the relevant residues is shown.

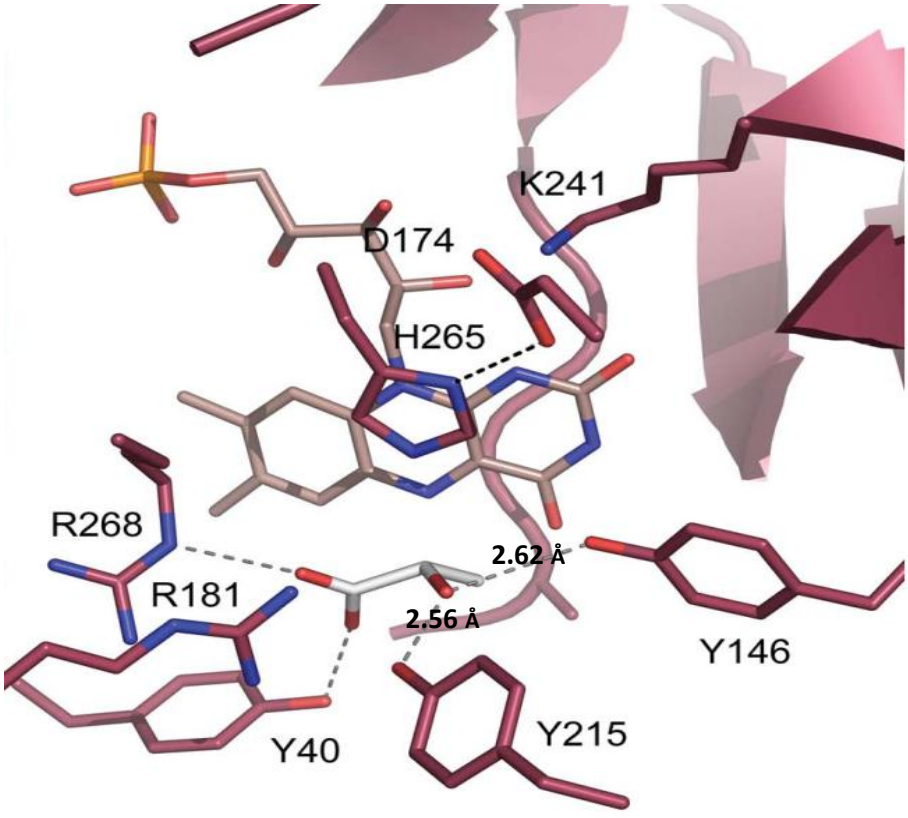

Figure 1-4 **Active site of L-lactate oxidase with L-lactate as substrate and the cofactor FMN (Leiros et al. 2006)**

2. Materials and methods

2.1. Site-directed mutagenesis

Site-directed mutagenesis to construct two LOX mutants Y215F and Y215H was conducted by a Two-stage PCR reported by Wang et al. (1999). The sequences of the used primers and their melting points are listed in Table 2-1.

Table 2-1 Sequence of primers used for site-directed mutagenesis

Primer	Sequence	T_m / °C
Y215Ffw	5'-TATCTTCGGTGˇCTAGCAAACAAAAAATCTCACCAAGAG-3'	62.3
Y215Frev	5'-GTTTGˇCTAGCACCGAAGATATTGTTTAATGACATACCTTCTGCTG-3'	63.8
Y215Hfw	5'-CAATATCCACGGTGˇCTAGCAAACAAAAAATCTCACC-3'	62.2
Y215Hrev	5'-GTTTGˇCTAGCACCGTGGATATTGTTTAATGACATACCTTCTG-3'	63.1

DNA sequence responsible for desired mutation

NheI restriction site

Beginning with two separate primer extension reactions – one for each forward and reverse primer – 1.5 µL of 10 pmol/µL primer (Integrated DNA Technologies) and approximately 200 ng pLO-1 (Roche Diagnostics) as plasmid template were incubated with 5 µL of 10x *PfuUltra*^{TM} buffer (Promega), 5 µL of 2 mM dNTP mix (Fermentas), 36.5 µL H_2O and 0.04 U *PfuUltra*^{TM} polymerase (Promega) for amplifying DNA at following conditions: heat denaturation at 95 °C for 1 minute, 4 treatment cycles, each consisting of 95 °C for 50 seconds, 57 °C for 50 seconds and 68 °C for 9 minutes, followed by 68 °C for 7 minutes and cooling at 4 °C. Afterwards 25 µL of each reaction – forward and reverse – were combined and the PCR temperature program was performed as above, but with 18 instead of 4 treatment cycles.

Afterwards template DNA was digested with 10 U *DpnI* restriction endonuclease (Fermentas) incubated at 37 °C for 1 hour. Plasmid DNA was transformed into electro competent *E. coli* BL21 (DE3) cells. After regeneration in SOC-Medium at 37 °C for 1 hour the cells were incubated on preheated LB-amp plates at 37 °C overnight.

Cells carrying the mutation were verified after plasmid isolation with a Miniprep-Kit (Promega Wizard® Plus SV Minipreps DNA Purification System) by *NheI* restriction. Restriction was conducted with 2 parts of the respective plasmid, 1 part restriction enzyme *NheI* and 10 x respective buffer (1 : 1) both from Fermentas, as well as 2 parts of H_2O. Reaction mixture was incubated at 37°C for 2 hours and subsequently heated at 75 °C for 5 minutes to inactivate the

restriction enzyme. The digested plasmid fragments were separated via agarose gel electrophoresis and mutants carrying a *NheI* restriction site could be differed from other plasmids, the wild type respectively. For agarose gel electrophoresis 6x Loading Dye (Fermentas) was added to the digested plasmid reaction mixture and transferred on 1 % agarose gel treated with ethidium bromide. Running buffer was 1 mM TEA and separation occurred at 80 V. Afterwards lanes were visualized with UV light.

DNA sequencing for verifying positive mutants was conducted by AGOWA.

2.2.Protein expression and cultivation

2.2.1. Expression and cultivation in fermenter

E. coli BL21 (DE3) cells harboring the plasmid containing the Y215F mutant gene were grown overnight as starter culture (0.55 % glucose monohydrate, 1 % peptone, 0.5 % yeast extract, 0.5 % NaCl, 0.1 % NH_4Cl, 0.025 % $MgSO_4*H_2O$, 100 µL/L polypropylene glycol), 0.3 % K_2HPO_4, 0.6 % KH_2PO_4, $0.2*10^{-3}$ % thiamine, $115*10^{-3}$ % ampicillin and $0.4*10^{-3}$ % $FeSO_4*7\ H_2O$, $0.1*10^{-3}$ % $MnSO_4*H_2O$, $0.04*10^{-3}$ % $CoCl_2$, $0.015*10^{-3}$ % $CuSO_4*5\ H_2O$, $0.01*10^{-3}$ % H_3BO_3, $0.02*10^{-3}$ % $ZnSO_4*7\ H_2O$, $0.02*10^{-3}$ % $Na_2MoO_4*2\ H_2O$ and $0.04*10^{-3}$ % $FeCl_3$ in 5 M HCl). The main culture (same medium as for the starter culture with a 4-fold higher amount of glucose monohydrate) was inoculated to an OD_{600} of 0.5. Temperature, stirring, pH and oxygen partial pressure in the B. Braun Biotech International Biostat®C, Type CT5-2 fermenter were controlled and adjusted automatically. pH was balanced at pH 7.0 with 2 M KOH and 1 M H_3PO_4, the pO_2 was fixed to a minimum of 40 %. The cells were grown at 37 °C before induction. At an OD_{600} of approximately 2 IPTG was added to a final concentration of 0.25 mM. The medium was supplemented with 115 mg/L ampicillin. Upon induction the cells were cultured at 30 °C. Cells were harvested, when the level of glucose was lower than 1 mg/mL (Diabur Test 5000, Roche Diagnostics). The pellet was suspended in 50 mM potassium phosphate buffer at pH 7.0 and stored at -25 °C.

2.2.2. Expression and cultivation in flasks

80 mL of LB-amp medium (10 g/L peptone, 5 g/L NaCl, 5 g/L yeast extract, 115 µg/L amp) were inoculated with *E.coli* BL21 (DE3) carrying the plasmid with the respective mutation (Y215F or Y215H) and shaken overnight at 37 °C with 130 rpm. The onc was used to generate glycerol stocks (final concentration of 10 % glycerol in the stock) which were stored at -70 °C and to inoculate 200 mL LB-amp medium in a 1 L flask to a starting OD_{600} of 0.1. Cells were grown to an OD_{600} of approximately 0.7-0.8 and then induced with IPTG to a final concentration of 250 µg/L. After 4 hour of incubation at 30 °C the cells were harvested by centrifugation at 5000 rpm and 4 °C for

30 minutes. Cells were resuspended in 50 mM potassium phosphate buffer at pH 7.0 and stored at -25 °C before further processing.

2.3.Protein purification

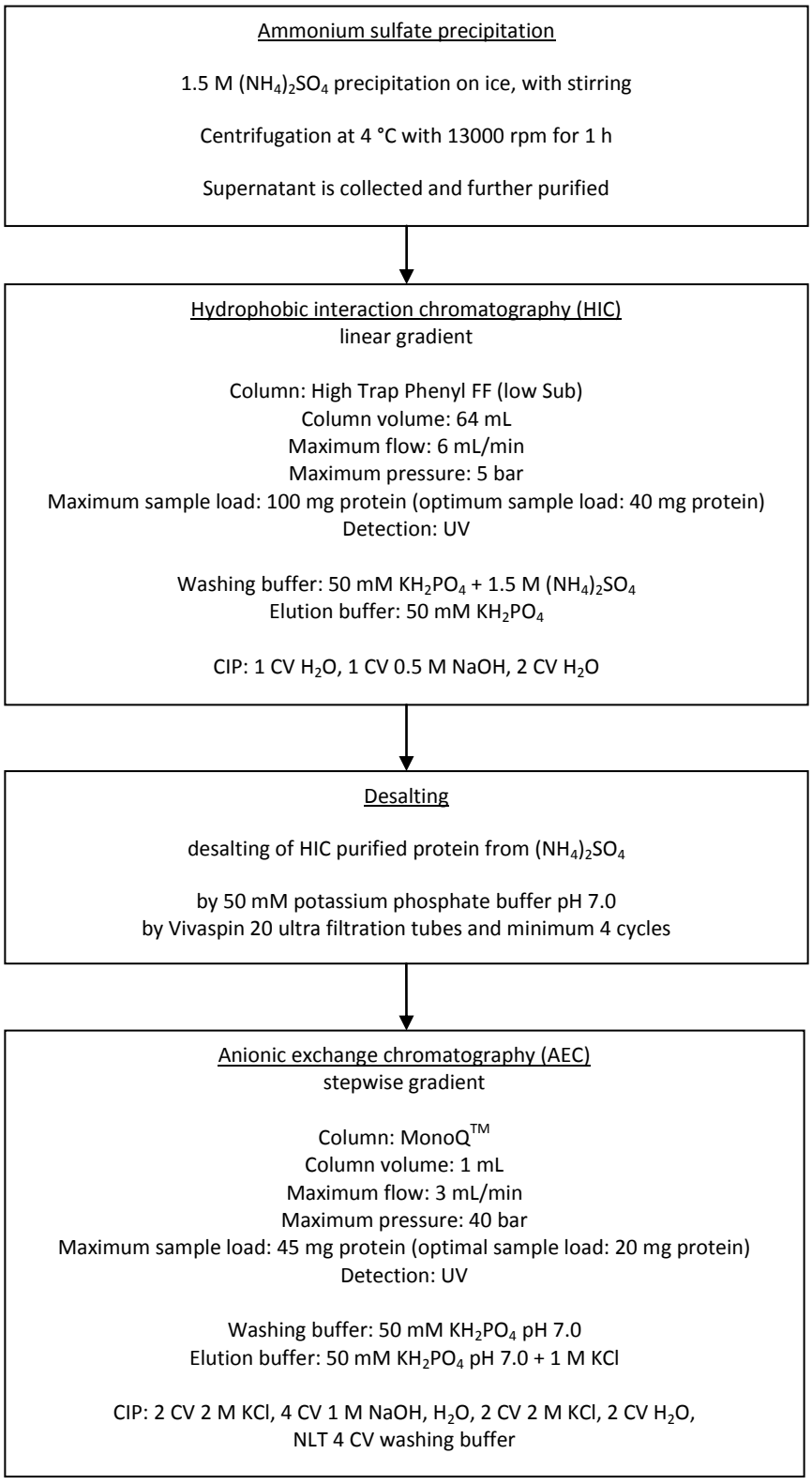

Figure 2-1 **Purification procedure including all possible steps**

Figure 2-1 shows the protein purification steps and conditions.

Cells were disrupted by French pressing. The crude extract was obtained by centrifugation. After precipitation in the presence of 1.5 M $(NH_4)_2SO_4$ at 4 °C by dropwise adding of a 3 M $(NH_4)_2SO_4$ solution and the removal of the precipitate by centrifugation, the L-lactate oxidase was purified by hydrophobic interaction chromatography using a Phenyl Sepharose 6 Fast Flow (High Sub) column (GE Healthcare Life Sciences) and an Äkta FPLC system (Amersham Biosciences). The protein was loaded on the column equilibrated with 50 mM potassium phosphate buffer at pH 7.0 and eluted at 25 °C with a linear increasing salt concentration with 50 mM potassium phosphate buffer containing 1.5 M ammonium sulfate at pH 7.0 and with a flow rate of lower than 6 mL/min and detection at 280 nm. Fractions containing significant amounts of active protein as determined with the below described spectrophotometric enzymatic assay were pooled and purity was verified by SDS-PAGE. Several HIC runs were conducted. Flow rate was for all runs between 2 and 6 mL/min, dependent on occurrent pressure and the sufficiency of the CIP runs. Protein solution was then desalted by repeated cycles of concentration and dilution using ultrafiltration devices (Vivaspin 20, 10 kDa cutoff, Vivascience AG, Hannover, Germany) and stored in 50 mM potassium phosphate buffer at - 25 °C until further processing.

Y215F mutant, expressed in flasks, as well as Y215H mutant were further purified with anion exchange chromatography (AEC) because of unsatisfying purity detected by SDS-PAGE. The desalted HIC purified protein was loaded on the MonoQ™ column and eluted with a stepwise increasing chloride anion concentration with a 50 mM phosphate buffer containing 1 M KCl, pH 7.0.

SDS-PAGE was used to verify impurity removal after each purification step. Therefore SDS PhastGel™ and buffer strips supplied by GE Healthcare were used. The samples were diluted to equal final concentrations and dissociation buffer was added at the ratio of 1:1. Protein was denaturated at 95 °C for approximately 2 minutes. Separation on the polyacrylamid gel was run on Phast system (Amersham Biosciences). Staining was achieved with Dying solution and stirring for 1 hour. Afterwards the gel was moved to Destain solution for the same time and conditions. In the end the gel was stirred over night in a Preserve Solution.

2.4.Assays

2.4.1. Determination of protein concentration

Protein concentration was determined by Bradford protein quantification assay (Roti® Quant, Carl Roth GmbH + Co KG) and measured photometrically at 595 nm. BSA was used as reference.

2.4.2. Determination of specific activity

The enzymatic activity of the LOX was determined using a standard enzymatic spectrophotometric assay (Sigma) described in literature (Maeda-Yorita et al 1995). The assay is a coupled assay. Hydrogen peroxide formed from L-lactate and oxygen by the LOX as catalyst, is in the second reaction converted into water and quinonediimine dye, which is proportional to the hydrogen peroxide concentration and is detected photometrically at 565 nm.

Both reactions are listed below and described as reaction 1 and 2 for simplification of subsequent explanations.

Reaction 1: L-lactate + O_2 $\xrightarrow{\text{LOX}}$ pyruvate + H_2O_2

Reaction 2: 2 H_2O_2 + 4-aminoantipyrine + N,N-dimethylaniline $\xrightarrow{\text{POD}}$ quinonediimine dye + H_2O

10 µL LOX appropriately diluted in 50 mM potassium phosphate buffer or H_2O were added to a coupled assay solution containing 40 mM 3,3-dimethylglutaric acid, 2.5 units peroxidase, 1.5 mM 4-aminoantipyrine, 0.04 v/v% N,N-dimethylaniline and 50 mM L-lactate to a total volume of 0.5 mL reaction mixture at pH 6.5. After a reaction time of 10 minutes at 37 °C 1 mL 0.25 w/v % dedecylbenzenesulfonic acid solution (DBS) was added to stop the reaction. The absorbance was measured spectrophotometrically at 565 nm with a Varian Cary® 50 Bio UV-Visible Spectrophotometer at RT and reaction rate v was calculated with Equation 2-1.

$$v = \frac{A_{565nm} * V_{assay} * df}{(\varepsilon * cf * t * V_{enzyme})}$$ **Equation 2-1**

where A_{565nm} is the measured absorbance at 565 nm, V_{assay} the total volume of the assay, df the dilution factor of the enzyme, ε the millimolar extinction coefficient of quinonediimine (35.33 $mM^{-1}cm^{-1}$), cf the conversion factor based on the fact that one mole of H_2O_2 produces half a mole of quinonediimine, t the time of the assay and V_{enzyme} the volume of the enzyme.

Specific activity was gained by considering the enzyme concentration (see Equation 2-2).

$$specific\ activity = \frac{v}{c}$$ Equation 2-2

where v is the reaction rate and c the enzyme concentration.

2.4.3. Determination of enzyme kinetics

For kinetic measurements the described enzymatic assay was performed with about ten various substrate concentrations of 1 mM - 50 mM. Besides L-lactate glycolic acid, L-2-hydroxy-3-methylbutyric acid, L-2-hydroxy-isocaproic acid, L-2-hydroxy-butyric acid and L-mandelic acid were used as substrates. Reaction rate v was calculated with Equation 2-1, K_M and v_{max} values were obtained by a non-linear fit of the Michaelis-Menten equation (see Equation 2-3) and in the case of substrate inhibition of Equation 2-4 to the reaction rates at different substrate concentrations with SigmaPlot® (version 11.0). k_{cat} values were calculated on the basis of enzyme concentrations (see Equation 2-5).

$$v = v_{max} * \frac{[S]}{K_M + [S]}$$ Equation 2-3

$$v = v_{max} * \frac{[S]}{(K_M + [S] * (1 + \frac{S}{KIS})}$$ Equation 2-4

$$k_{cat} = \frac{v_{max}}{[E]}$$ Equation 2-5

where v represents the reaction rate, v_{max} the maximum rate, [S] the substrate concentration, K_M the Michaelis constant, K_{IS} the dissociation constant of the enzyme-inhibitor-substrate complex, k_{cat} the turnover number and [E] the enzyme concentration.

3. Results

3.1.Site-directed mutagenesis

The integrated restriction site for *NheI* was used to identify positive mutants. One original *NheI* restriction site of the plasmid is at 1235 bp and the integrated restriction site was at 950 bp. Thus after digestion of the vector (4062 bp) by the *NheI* restriction enzyme two fragments – one with about 3800 bp and the other with approximately 300 bp – were generated. Agarose gel electrophoresis was used to identify mutants. The DNA fragments were separated by length and their size could be estimated. In Figure 3-1 a picture of the agarose gel of positive LOX mutants is shown. GeneRuler™ 100 bp Plus DNA Ladder from Fermentas was used as DNA size marker. The highlighted lanes of Y215H as well as Y215F were of positive mutants, which were subsequently expressed in *E. coli*. As expected the lanes of the mutants were slightly lower than the lane of the wild type (WT). The second expected lanes of the mutants at about 300 bp were not visible on the gel. However the mutants were positive and therefore successful mutation had occurred.

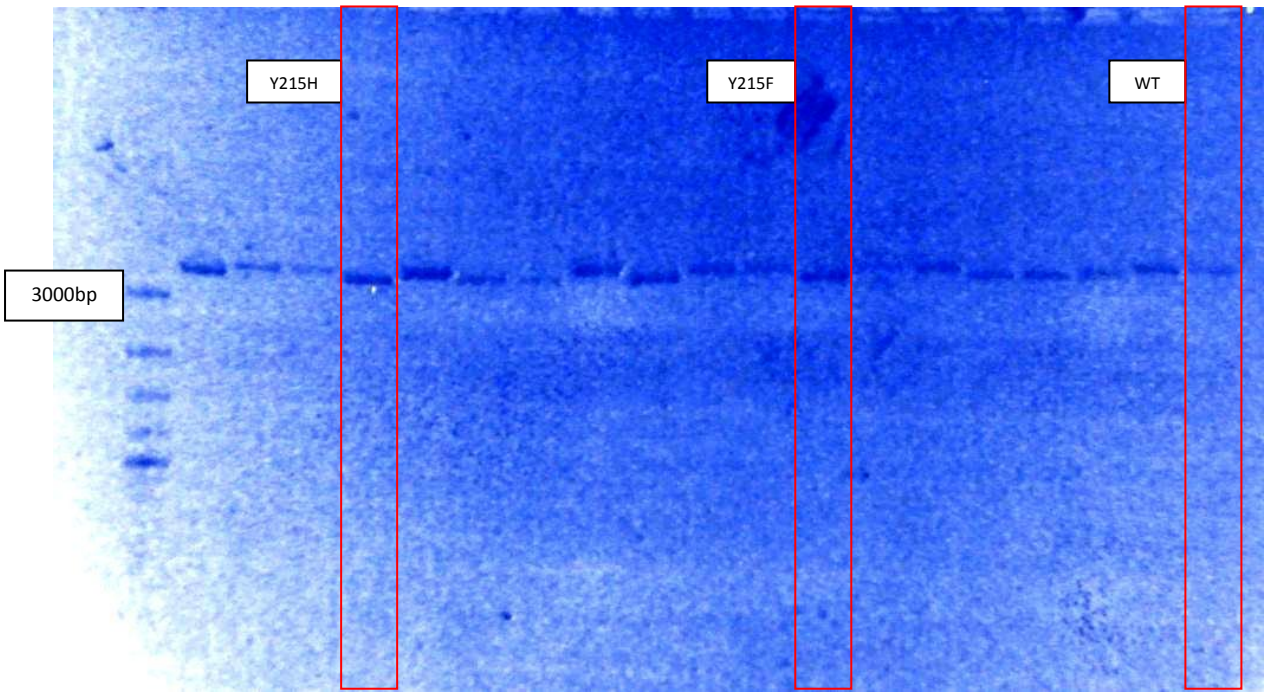

Figure 3-1 **Agarose gel of *NheI* digested LOX plasmids containing respective mutations; highlighted lanes were used for further processing (lane 1: DNA ladder, lane 2-10: Y215H, lane 11-19: Y215F plasmids, lane 20: WT)**

3.2.Protein expression and purification

In Table 3-1 specific activities and recovery rates for Y215F and Y215H expressed in flasks, as well as for Y215F expressed in fermenter, are listed.

Table 3-1 **Purification of L-lactate oxidase mutants**

Mutant	Procedure	Specific activity / U/mg	Recovery / %
Y215F	Crude extract	0.30	100
	(NH_4SO_4) precipitation	0.74	88
	HIC	30.1	43
	AEC	75.6	9
Y215F(ferm)	Crude extract	5.3	100
	(NH_4SO_4) precipitation	9.5	88
	HIC	59.9	26
Y215H	Crude extract	0.25	100
	(NH_4SO_4) precipitation	0.68	89
	HIC	1.77	42
	AEC	13.4	10

Activity of Y215F expressed in flasks was after HIC purification only half of the specific activity of Y215F expressed in fermenter. It might be referred to different conditions during expression and cultivation in flasks compared to those in fermenter. Remaining impurities after HIC purification of Y215F are illustrated in Figure 3-2 (highlighted lanes), showing the gel of the Y215F purification intermediates after expression in flasks and in fermenter. Because of the big loss of protein during AEC for Y215H and Y215F (expressed in flasks) it was decided to skip this purification step for Y215F (expressed in fermenter), also because of the sufficient purity seen on the gel. The specific activity for Y215F expressed in fermenter after HIC purification was 20 % below the specific activity of the HIC and AEC purified Y215F mutant expressed in flasks.

Figure 3-2 and Figure 3-3 show SDS gels of the purification intermediates for Y215F (and Y215H mutant.

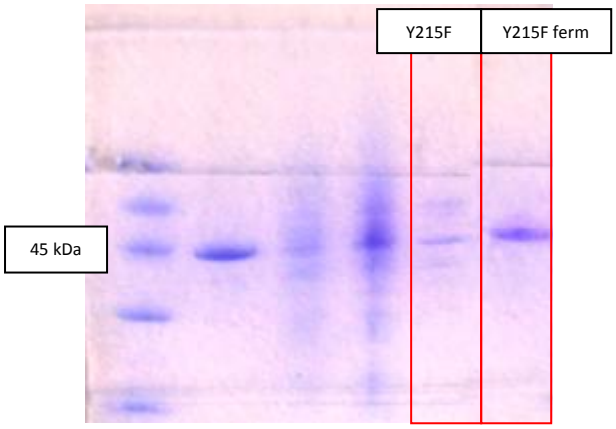

Figure 3-2 **Purification of Y215F mutant documented by SDS-PAGE; lane 1: low molecular weight marker, lane 2: WT, lane 3: crude extract of Y215F (expressed in flasks), lane 4: after $(NH_4)_2SO_4$ precipitation of Y215F (expressed in flasks), lane 5: after HIC purification of Y215F (expressed in flasks), lane 6: after HIC purification of Y215F (expressed in fermenter)**

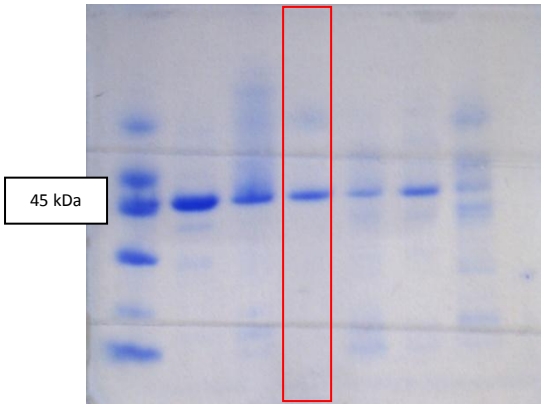

Figure 3-3 **Purification of Y215H mutant documented by SDS-PAGE, highlighted lanes were used for further processing (lane 1: low molecular weight marker, lane 2: WT, lane 3 und 4: Y215H after AEC, lane 5-7: Y215H after HIC)**

3.3.Kinetic measurements with L-lactate and alternative substrates

Kinetic characteristics for L-lactate and a range of other L-α-hydroxy acids, which were converted into the corresponded α-keto acid, are listed in Table 3-2. Measurements were performed using the described assay in section 2.4.2. For the present measurements Y215F und Y215H mutants, which were expressed in flasks and HIC as well as AEC purified, were used. The wild type was supplied by Roche Diagnostics.

Table 3-2 Substrate specificity for LOX mutants

Substrate	Mutant	Specific activity / U/mg	k_{cat} / s^{-1}	K_M / mM	k_{cat}/K_M / $s^{-1}mM^{-1}$	K_{IS} / mM
L-(+)-lactic acid	wild type Y215F Y215H	204 ± 1 75.6 ± 1.8 13.4 ± 0.2	140 ± 1 51.7 ± 1.2 9.12 ± 0.1	0.83 ± 0.03 0.09 ± 0.01 0.85 ± 0.04	167 561 10.7	- 112 ± 11 -
glycolic acid	wild type Y215F Y215H	1.44 ± 0.02 0.27 ± 0.01 0.40 ± 0.02	0.98 ± 0.01 0.19 ± 0.01 0.27 ± 0.01	0.44 ± 0.06 0.22 ± 0.01 1.16 ± 0.33	2.2 0.6 0.2	117 ± 30 976 ± 280 -
L-(+)-2-hydroxy-3-methylbutyric acid	wild type Y215F Y215H	0.25 ± 0.01 n.d. n.d.	0.18 ± 0.01 n.d. n.d.	3.30 ± 1.30 n.d. n.d.	0.1 n.d. n.d.	- - -
L-2-hydroxy-isocaproic acid	wild type Y215F Y215H	1.60 ± 0.17 3.75 ± 0.04 0.85 ± 0.03	1.10 ± 0.12 2.56 ± 0.03 0.58 ± 0.02	0.43 ± 0.05 0.71 ± 0.04 0.32 ± 0.07	1.0 4.8 1.8	- - -
L-2-hydroxy-butyric acid	wild type Y215F Y215H	2.00 ± 0.02 11.3 ± 1.3 1.18 ± 0.03	1.38 ± 0.01 7.72 ± 0.89 0.81 ± 0.02	0.43 ± 0.05 1.47 ± 0.26 0.70 ± 0.07	1.3 5.4 1.2	- - -
L-(+)-mandelic acid	wild type Y215F Y215H	0.14 ± 0.00 n.d. n.d.	0.10 ± 0.00 n.d. n.d.	0.48 ± 0.10 n.d. n.d.	0.2 n.d. n.d.	- - -

Compared with the wild type the specific activity of Y215F for L-lactate is lowered by a factor of 2.7, for Y215H by a factor of approximately 15. The lacking hydrogen bond for stabilization of the anionic form of the substrate in Y215F might be the reason for the lower specific activity compared to the wild type. But Tyr^{215} might not be involved directly in substrate conversion. If it was involved mutation would probably lead to a much lower activity or to an inactive enzyme. Steric properties of histidine compared to tyrosine might be the reason for the low specific activity for L-lactate in Y215H. Furthermore a lowered K_M in Y215F by a factor of approximately 9 is observed. The lacking hydroxyl group might have a positive influence on enzyme-substrate affinity. Although the k_{cat} of Y215F is lower compared to the wild type, the low K_M value leads to a higher catalytic efficiency by the factor of 3.4 for Y215F. In addition substrate inhibition occurs at higher substrate concentrations in Y215F. The removal of the hydroxyl group by the replacement of tyrosine with phenylalanine

might induce a second substrate binding site, which further leads to inhibition of substrate conversion (Bisswanger 2002).

The specific activity of Y215H for glycolic acid is lowered by a factor of 3.5 compared to the wild type and the K_M is higher than the K_M of the wild type, which could be considered as a positive effect for the use of Y215H in biosensors used in medical diagnosis, without regard to the as well low specificity for L-lactate. Specific activity for glycolic acid is decreased in mutant Y215F, whereas K_M is lowered by a factor of 2. Thus enzyme-substrate affinity for Y215F is higher compared to the wild type. Furthermore substrate inhibition at higher glycolic acid concentrations has been observed in Y215F, as well as in the wild type. That differs from Y215H, where no substrate inhibition at higher glycolic acid concentration occurs, which might result from the steric properties of Y215H.

Specific activity, k_{cat} and K_M were changed by mutation at Tyr^{215} for all determined substrates. Kinetic data of L-mandelic acid and L-2-hydroxy-3-methylbutyric acid for Y215F and Y215H could not be determined because values were below the detection limit. Specific activity for longer chain L-α-hydroxy acids, branched and linear, is very low for the wild type. This might result from steric conditions in the active site. An example is given in literature, where Ala^{95} is replaced by a glycine, resulting in a 4750-fold higher k_{cat} for L-mandelic acid compared to the wild type (Yorita et al. 1996). Therefore the change of steric properties in the active site due to the mutations might also be a reason for the lowered specific activity of Y215F and Y215H for longer chain L-α-hydroxy acids.

Table 3-3 Activity of Y215F expressed in flasks and in fermenter

Substrate	**Mutant**	**Specific activity / U/mg**	**k_{cat} / s^{-1}**	**K_M / mM**	**k_{cat}/K_M / $s^{-1}mM^{-1}$**
L-(+)-lactic acid	Y215F	75.6 ± 1.8	51.7 ± 1.2	0.09 ± 0.01	561
	Y215F(ferm)	59.9 ± 1.5	41.0 ± 1.0	0.11 ± 0.01	364

Table 3-3 kinetic data for L-lactate in Y215F expressed in flasks and in fermenter are compared. Y215F expressed in flasks was purified by HIC and AEC after $(NH_4)_2SO_4$ precipitation, whereas Y215F expressed in fermenter was only HIC purified. Specific activity for L-lactate in Y215F expressed in fermenter is 20 % below the activity observed in Y215F expressed in flasks.

4. pH studies

On the basis of Sobrado et al. (2003) pH studies for the LOX mutants, as well as the wild type could lead to information about the reaction mechanism of the L-lactate oxidase in detail. On the basis of k_{cat} and k_{cat}/K_M at different pH values the pK(s) of the wild type and Y215F could be determined and could give information of the role of Tyr^{215} in substrate binding and conversion.

As already mentioned in section 1.1 two possible mechanism for the reductive half-reaction of the related L-α-hydroxy acid oxidizing flavoenzymes are postulated – on the one hand a mechanism, in which a carbanion is formed and on the other hand a hydride transfer mechanism. As seen in Figure 1-3 the orientation of the substrate is different for both supposed mechanism. As the catalytic histidine (His^{265} in LOX) abstracts the α-proton of the substrate to form a carbanion, the α-hydrogen points toward the histidine in the carbanion mechanism. In hydride transfer mechanisms the proton of the α-hydroxyl group is abstracted by the base and the α-proton is directly transferred as a hydride to the cofactor. In this case the hydroxyl group points towards the histidine (Furuichi et al. 2008).

Of particular interest for the present work are the considerations of Sobrado et al. (2003) to the Tyr^{254} residue in flavocytochrome b_2. Flavocytochrome b_2 of *Saccharomyces cerevisiae* has been the most studied α-hydroxy acid oxidizing FMN-dependent enzyme. It catalyzes the oxidation of L-lactate to form pyruvate with a subsequent electron transfer to cytochrome c aided by FMN and heme b_2 cofactors. Tyr^{254} in flavocytochrome b_2 is a conserved amino acid within the enzyme family and correlates with Tyr^{146} in L-lactate oxidase. As already mentioned Tyr^{146} as well as Tyr^{215} in LOX might interact with the hydroxyl group of the substrate because of their substrate proximity (Sobrado et al. 2003, Umena et al. 2006).

According to Sobrado et al. (2003) there are different considerations of the role of Tyr^{254} in flavocytochrome b_2, whether the carbanion or the hydride transfer mechanism occurs. If the carbanion mechanism occurred the tyrosine would interact as a base to abstract hydrogen of substrate's α-carbon and it would have to be in the anionic form at physiological conditions to have the facility to interact as a base. In the hydride transfer the tyrosine would orient the substrate for hydride transfer by the formation of a hydrogen bond between the substrate and the phenol of the tyrosine, which would be most compatible with a neutral tyrosine. pH studies, as well as solvent isotope effects and rapid reaction kinetics by stopped flow measurements with the flavocytochrome b_2 mutant Y254F by Sobrado et al. (2003) supported the hydride transfer as mechanism of the reductive half-reaction of flavocytochrome b_2 and affirmed the role of Tyr^{254} as stabilizer of the substrate (Dubois et al. 1990, Sobrado et al. 2003).

Kinetic studies on the flavocytochrome b_2 mutant Y254F reported by Dubois et al. (1990) showed a decrease of the rate of L-α-hydroxyl acid oxidation by 1-2 magnitude orders compared to the wild type.

Because of the proximity to the substrate of Tyr^{215} and Tyr^{146} (see also Figure 1-4) in L-lactate oxidase, experiments to find out more about the role of Tyr^{215} are of big interest, but have not been reported yet. In contrast to Tyr^{146} Tyr^{215} is a non-conserved amino acid, which leads to the assumption that this residue might be the reason for the unique properties of L-lactate oxidase - i.e. specificity for L-lactate and, compared to L-lactate monooxygenase, the formation of pyruvate and hydrogen peroxide instead of acetate, carbon dioxide and water (Maeda-Yorita et al. 1995). To understand the role of Tyr^{215} pH studies were conducted.

Another aspect of pH studies of active site mutants is the possible change of the orientation of residues at different pH values. Experiments according to this topic were performed by Furuichi et al. (2008). By protein crystallization they found out that at pH 4.5 the catalytic His^{265} in L-lactate oxidase is flipped out during the reductive half-reaction. This probably results from the protonation of His^{265}. The pK value of histidine is around 6 and therefore at pH 4.5 histidine is likely to exist as the di-protonated form. Also at pH 8.0 there was a change in conformation observed, but not as significant as for His^{265} at pH 4.5. The pH 8.0 histidine remains closer to the substrate, whereas at pH 4.5 the histidine flips away from the substrate and returns during oxidative half-reaction, i.e. the entrance of oxygen, to be deprotonated and to function as catalyst for FMN reoxidation and hydrogen peroxide forming. Furuichi et al. (2008) did not perform any kinetic measurements in this context, but the facts of changing conformation of single active site residues by the change of the pH are significant and could result in changing of the reaction mechanism and kinetic parameters as well (Furuichi et al. 2008).

4.1.Pre-experiments and methods

In this section methods and (pre-)experiments, which were performed to find a method for the measurement of the L-lactate oxidase activity at different pH values, are discussed. Pre-experiments are described and analyzed, whether they worked or not.

Following experiments were conducted with mutant Y215F. Two different approaches to determine the activity were adopted - one to measure the oxygen consumption and the other to measure the formation of hydrogen peroxide, one of the products.

4.1.1. Oxygen measurement

Method

According to Sobrado et al. (2003) following buffers were used to measure the oxygen consumption for pH studies: 50 mM BisTris for pH 5.0-7.0, 150 mM HEPES for pH 7.0-8.5 and 50 mM ethanolamine for pH 8.5-10.0. Buffer and substrate solution were combined to a defined final concentration of L-lactate from 0.1 mM to 50 mM and preheated at 37 °C using a water bath. After the addition of enzyme the consumption of oxygen was monitored with an oxygen sensor at a temperature of 37 °C, which was assumed to be constant by using a heating jacket assembly. Kinetic measurements were conducted for 10 various substrate concentrations and at pH 5-10.

Results and resume

Because of the poor reproducibility of the measurements this method was not used for the pH studies. A reason for the poor reproducibility of the method might be the temperature, which was difficult to keep constant at 37 °C with the set-up used and described above.

4.1.2. Hydrogen peroxide measurement by continuous assay

Because of the bad reproducibility of the measurement of oxygen consumption by an oxygen sensor (see section 4.1.1), the second approach - measurement of enzyme activity by the formation of hydrogen peroxide – was adopted. Thus the enzymatic assay mentioned in section 2.4.2 was optimized for the activity measurement at pH 5-10. These experiments are described in the following section.

4.1.2.1. Buffer

First experiments were done to find adequate buffers for the assay for the entire range of pH values. Buffers can influence the activity as well as the stability of the enzyme. Thus LOX activities in different buffers at the same pH value were compared.

Method

The enzymatic assay described in section 2.4.2 was conducted at pH 6.5 and pH 7.0. At pH 6.5 the assay was performed with 40 mM DMGA, 10 mM BisTris and a multiple component buffer (multiple-component buffer 1) consisting of 10 mM MES, 10 mM HEPES and 20 mM ethanolamine (final concentrations in reaction mixture). At pH 7.0 the kinetic measurements in 30 mM HEPES were compared to those with 10 mM BisTris.

Results

The results of activity measurement at different buffer conditions are listed in Table 4-1 (for pH 6.5) and Table 4-2 (for pH 7.0).

Table 4-1 **Specific activity of the LOX at pH 6.5 at different buffer conditions**

Buffer	Specific activity / U/mg
40 mM DMGA	59.9
10 mM BisTris	33.2
Multiple-component buffer 1 (10 mM MES, 10 mM HEPES, 20 mM ethanolamine)	25.5

Table 4-2 **Specific activity of the LOX at pH 7.0 at different buffer conditions**

Buffer	Specific activity / U/mg
30 mM HEPES	48.8
10 mM BisTris	67.1

The results indicate that the measured activity and the formation of quinonediimine respectively, might be buffer-dependent. Unequal activity values were determined at same pH values but different buffers.

Resume

To gain representative activity values the same buffer has to be used for the entire pH range from pH 5 to pH 10. Because of the assumption that the ionic strength of the buffer influences the activity of the enzyme (Ellis et al. 1982) it was decided to use a multiple-component buffer with a final concentration in the assay solution of 10 mM MES, 10 mM HEPES and 20 mM ethanolamine and with constant ionic strength, which was adjusted by the addition of respective concentrations of NaCl.

4.1.2.2. Measurements at various pH values

To verify the suitability of the usage of a multiple-component buffer for the measurement of enzyme kinetics at different pH values, the enzymatic assay of section 2.4.2 was conducted with multiple-component buffer 1 instead of DMGA.

Method

Kinetic measurements were conducted as described in section 2.4.2 and 2.4.3 with multiple-component buffer 1 with a final concentration of 10 mM MES, 10 mM HEPES and 20 mM ethanolamine at pH 5 to pH 10.

Results

At high pH values, e.g. pH 9, the formed quinonediimine was degraded in a few minutes. Thus a representative photometrical measurement could not be conducted.

Resume

This method is not suitable to create an entire pH profile of the enzyme, because of the observed pH-dependent degradation of the dye. POD and quinonediimine might be pH-dependent under the present conditions (Corbett et al. 1969). Because of the parallel reactions of LOX and POD in the assay, namely a continuous experimental procedure, in this case the detected quinonediimine does not represent the actual conversion of L-lactate into hydrogen peroxide and pyruvate.

4.1.3. Hydrogen peroxide measurement by discontinuous assay

To avoid the effect of the pH on POD and quinonediimine (described in section 4.1.2.2), the enzymatic assay of section 2.4.2 was conducted in a discontinuous way. Reaction 1 was performed in multiple-component buffer with different pH values from 5 to 10, whereas reaction 2 was performed in 40 mM DMGA at pH 6.5.

Method

The enzymatic assay as described in section 2.4.2 was conducted in a discontinuous way. After the conversion of L-lactate into hydrogen peroxide by the LOX (in multiple-component buffer 1 at pH 5-10), the formed hydrogen peroxide was converted to quinonediimine by POD in a separate reaction mixture (at pH 6.5 in 40 mM DMGA). The concentration of quinonediimine was determined photometrically at 565 nm. To avoid further LOX-catalyzed conversion during the peroxidase reaction (reaction 2), a possibility to stop the activity of the LOX had to be found.

The subsequent experiments dealt with different possibilities to stop the LOX reaction before starting reaction 2. Considered possibilities were inhibition and thermal inactivation of the LOX.

4.1.3.1. LOX inhibition

Relevant inhibitors of the LOX and their K_I values are listed in Table 4-3 (Streitenberger et al. 2001, Maeda-Yorita et al. 1995).

Table 4-3 Relevant inhibitors of the LOX

Inhibitor	K_I / mM
Oxalate	0.5
D-lactate	9.04
Cibacron blue 3GA	0.00169
Sulfite	n.d.

Comments and resume

Oxalate and D-lactate are not adequate inhibitors for the LOX because of their high K_I values. Cibacron blue 3GA has a low K_I, but is pH- and time-dependent, especially at low concentrations. In addition it is a dye, which would influence the photometrical detection of quinonediimine (Streitenberger et al. 2001). Thus it is useless for pH studies. Sulfite reduces hydrogen peroxide to water and therefore it is not suitable for the assay.

In Literature L-mandelate and 2-hydroxybutyrate are mentioned as inhibitors as well, but they are also substrates for the LOX and therefore insufficient inhibitors (Streitenberger et al. 2001).

Because of the above mentioned reasons the relevant inhibitors cannot be used.

4.1.3.2. Thermal inactivation of the LOX

Methods

Measurement of oxygen consumption

Multiple-component buffer 1, pH 6.5 and 92 nM enzyme were incubated for various incubation times and at different temperatures (70 °C or 90 °C). After addition of 50 mM L-lactate the oxygen consumption was monitored with an oxygen sensor at 37 °C (see section 4.1.1).

Continuous monitoring of the formation of quinonediimine

To verify the results of the oxygen measurement a continuous photometrical measurement was conducted as well. Multiple-component buffer 1 and 0.16 nM LOX were incubated at 90 °C for 30 seconds, 1 and 2 minutes respectively. 5 mM L-lactate was added. Incubation time for the LOX reaction (reaction 1) was 14 minutes. Afterwards the residual components of the assay (see section 2.4.2) which are necessary for the formation of quinonediimine, were added. No DBS as stop solution was used, because the formation of quinonediimine was observed by continuous photometrical monitoring at 565 nm.

Results

Measurement of oxygen consumption

In Table 4-4 the resulting (rest) activities for 50 mM L-lactate are listed.

Table 4-4 **Activities of Y215F after thermal treatment**

Incubation temperature / °C	Incubation time (thermal treatment) / min	Activity (at 50 mM L-lactate) / U/mg
70	5	12.67
70	10	7.479
90	0.5	0
90	1.5	0
90	5	0
Reference (without thermal treatment)	-	22.86

An example of monitoring oxygen consumption after thermal treatment of the LOX at 90 °C for 30 seconds is displayed in Figure 4-1.

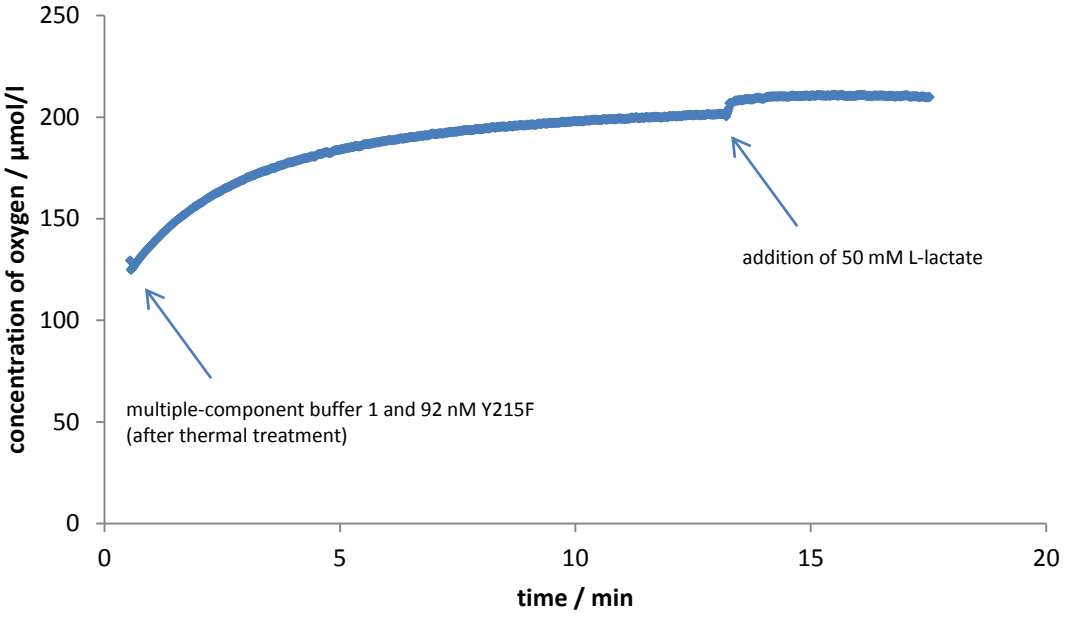

Figure 4-1 **Oxygen measurement after thermal treatment of the LOX**

The oxygen measurements show that there is a rest activity of the LOX after incubation at 70 °C for 5 or 10 minutes, but there is no visible rest activity after incubation at 90 °C for 30 seconds, 1.5 minutes or 5 minutes. This leads to the assumption, that it is possible to inactivate the LOX by incubation at 90 °C for at least 30 seconds.

Continuous monitoring of the formation of quinonediimine

In Figure 4-2 the formation of quinonediimine after the incubation of the enzyme at 90 °C for 30 seconds, 1 and 2 minutes is demonstrated. There is a continuous increase of the concentration of quinonediimine, which leads to the assumption that the LOX could not be completely inactivated by thermal treatment at 90 °C. Furthermore it can be observed that the longer the incubation time at 90 °C, the lower the measured absorption.

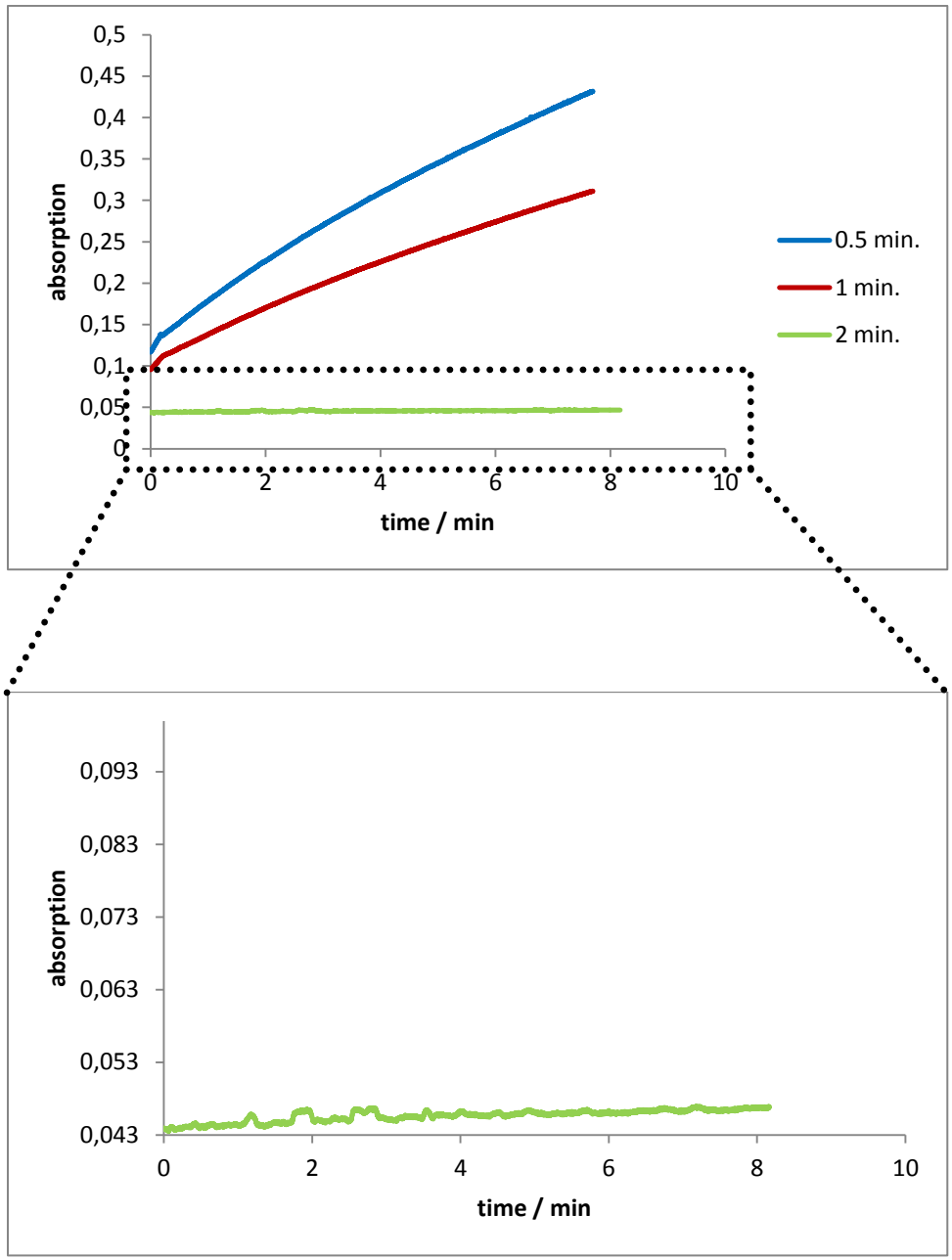

Figure 4-2 **Continuous photometrical measurement of the discontinuous assay after thermal treatment**

Resume

Contrary to the results of the oxygen measurements discontinuous assay measurements show that the LOX is still active after incubation at 90 °C for 30 seconds, 1 minute and 2 minutes. Therefore thermal inactivation is no suitable option for stopping the LOX activity. Furthermore it has been observed that the longer the incubation time at 90 °C, the lower the measured absorption. This could arise from instability of formed hydrogen peroxide at 90 °C (dependent on the incubation time).

4.1.4. Stability measurements of hydrogen peroxide

4.1.4.1. Determination of thermal stability

Because of the results of the previous section, experiments were performed to find out if hydrogen peroxide is stable at different assay conditions, i.e. continuous and discontinuous enzymatic assay and with and without thermal treatment at 90 °C.

Method

The assay was conducted in a continuous and a discontinuous (with and without thermal treatment at 90 °C) way (same conditions as described in section 2.4.2 and 4.1.3). The continuous assay was conducted with 0.08 nm enzyme, the discontinuous assay with 0.8 nM enzyme.

Furthermore reference measurements with added hydrogen peroxide at the same conditions were performed. Instead of L-lactate and LOX free hydrogen peroxide was added.

Conditions of the measurements are listed in Table 4-5.

Table 4-5 Used conditions and components the enzymatic assay

Assay		c (L-lactate/H_2O_2) / µM	Buffer	Incubation (LOX reaction) / min	Incubation (90 °C) / min
formed H_2O_2 (by LOX)	continuous	100	40 mM DMGA (pH6.5)	5	---
	discontinuous (without thermal treatment)		LOX-reaction: multiple-component buffer (pH 6.5)[3] POD-reaction: 40 mM DMGA (pH6.5)		---
	discontinuous (with thermal treatment[2])				0.5
added H_2O_2	continuous		40 mM DMGA (pH6.5)		---
	discontinuous (without thermal treatment)		LOX-reaction: multiple-component buffer (pH 6.5)[3] POD-reaction: 40 mM DMGA (pH6.5)		---
	discontinuous (with thermal treatment[2])				0.5

[1] the concentration for L-lactate for all measurements, where the formed H_2O_2 is analyzed and the concentration for H_2O_2, where H_2O_2 is added for reference studies

[2] thermal treatment at 90 °C

[3] 10 mM MES, 10 HEPES and 20 mM ethanolamine

The POD reaction (reaction 2) of all measurements is stopped by 1 mL DBS after 5 minutes (see Table 4-5) in the continuous assays and directly after adding all components of the POD reaction in the discontinuous assays. Afterwards the absorption is measured spectrophotometrically at 565 nm discontinuously.

Results

In Figure 4-3 results of the activity measurements at different assay conditions are illustrated.

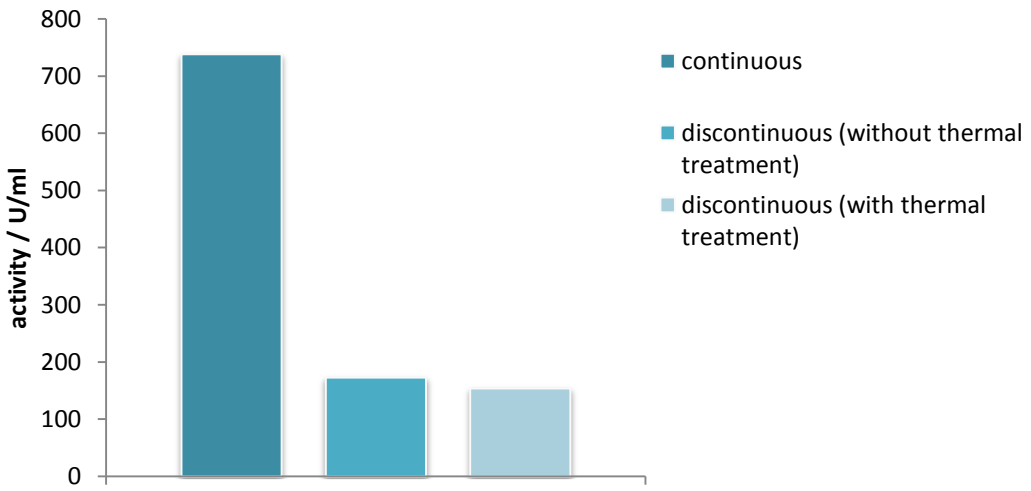

Figure 4-3 **Activity of the LOX at different assay conditions**

In Figure 4-4 the results of the reference measurements with added hydrogen peroxide are displayed.

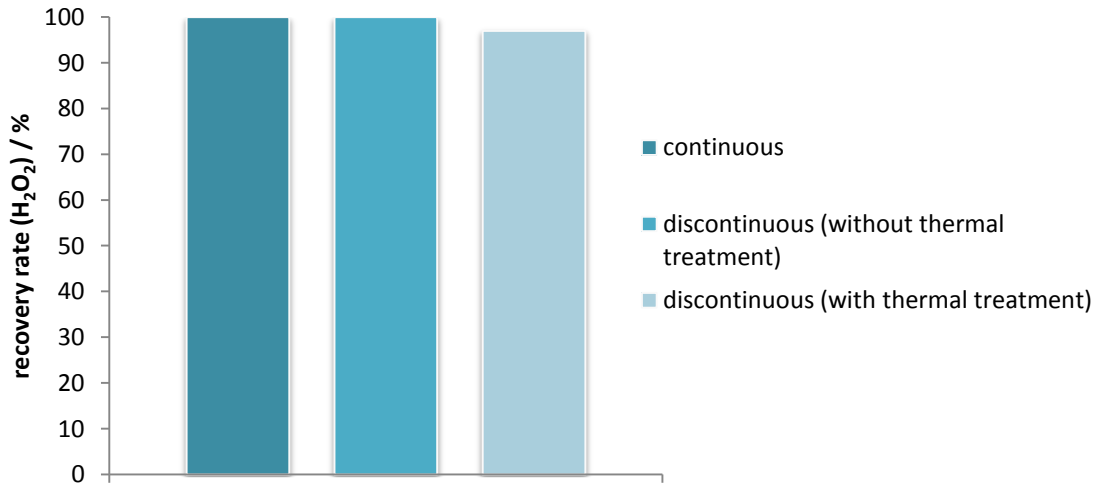

Figure 4-4 **Recovery rate of hydrogen peroxide at different assay conditions**

In contrast to the reference measurements with free hydrogen peroxide (see Figure 4-4) the activity values for the LOX differ between the continuous and the discontinuous assay measurements. The resulting activities of both discontinuous measurements are only about 20 % of the measured activity of the continuous assay. But, against expectations, there is almost no difference between the discontinuous assay with and without thermal treatment.

The reference measurements with hydrogen peroxide show that there is only a negligible decrease of hydrogen peroxide concentration caused by the incubation at 90 °C for 30 seconds.

Resume

There might be significant effects caused by the discontinuous enzymatic assay, which influence the activity of the LOX or the stability of hydrogen peroxide. Experiments, which were conducted to find out more about these effects, are described in the following section.

4.1.4.2. Determination of stability at different pH values

The discontinuous assay without thermal treatment was conducted to find out more about the effects of the discontinuous assay. Because thermal treatment did not lead to the desired complete LOX inactivation, it was not applied anymore in further experiments. The incubation time of the LOX reaction was varied to see possible impacts on measured concentration of quinonediimine due to reaction time of the LOX.

Method

The assay was performed as described in section 4.1.3, with the exception that measurements were conducted with 5-7 different times of incubation and at different pH values(pH 5.5 – 7) of the LOX reaction (reaction 1). The reactions were conducted with 5 mM L-lactate, with multiple-component buffer 1 and 8 nM Y215F mutant.

Results

The results of the measurements are illustrated in Figure 4-5.

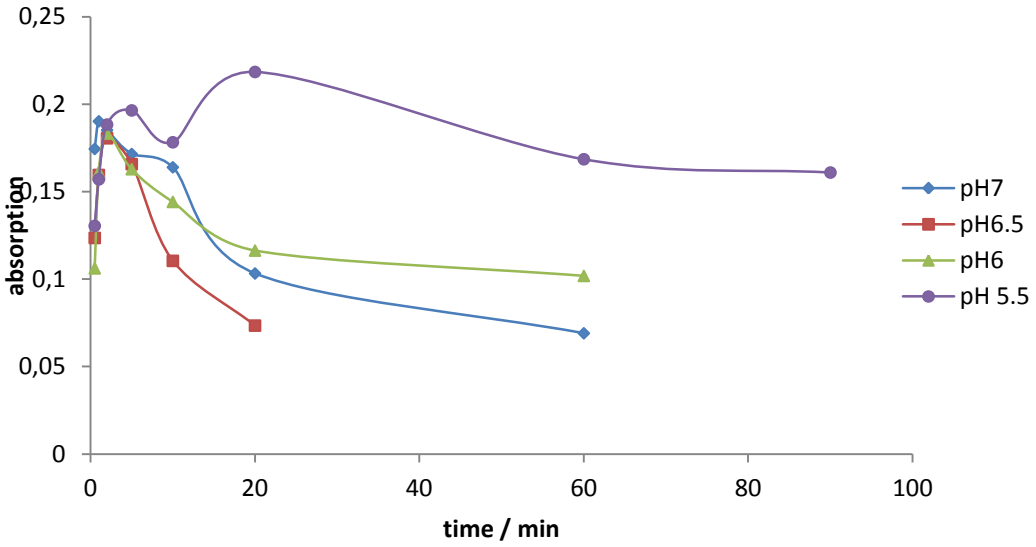

Figure 4-5 **Formation of quinonediimine at different pH values and incubation times**

After an observable increase of the absorption and concentration of formed quinonediimine dye respectively, in the beginning the absorption decreases with longer incubation time of the LOX, dependent on the pH value.

Resume

The decreasing concentration of quinonediimine during longer LOX incubation time leads to the assumption that a degradation of hydrogen peroxide takes place. In literature a possible reaction mechanism, which might occur, namely a peroxide- and pH-dependent decarboxylation of pyruvate, is described (Fox et al. 1995).

The experiments done on the discontinuous enzymatic assay show that it is not an adequate assay to compile an entire pH profile. First of all there was no way found to stop LOX activity after reaction 1. Furthermore the resulting concentration of quinonediimine was not proportional to the converted L-lactate due to the instability of hydrogen peroxide over time.

4.1.5. Optimization of continuous enzymatic assay

Because of the low suitability of the discontinuous assay for compiling a pH profile for the wild type and Y215F (see previous sections), experiments were performed to optimize the continuous assay. The intention was to find an adequate buffer in which reaction 1 and 2 can take place over a pH range from 5 to 10.

Method

The continuous assay was conducted as described in section 2.4.2 with 50 mM L-lactate and 80 pM enzyme. Three experiments with three different buffers at pH 6.5, i.e. 40 mM DMGA, multiple-component buffer 1 with 10 mM MES, 10 mM HEPES and 20 mM ethanolamine and multiple-component buffer 2 with 20 mM MES, 20 mM HEPES and 40 mM ethanolamine, were performed. After reaction time of 5 minutes, 1 mL DBS was added to stop the reactions and the absorption was continuously photometrically monitored at 565 nm.

Results

In Figure 4-6 absorption characteristics over time of quinonediimine formed during enzymatic assay reaction in different buffers are illustrated.

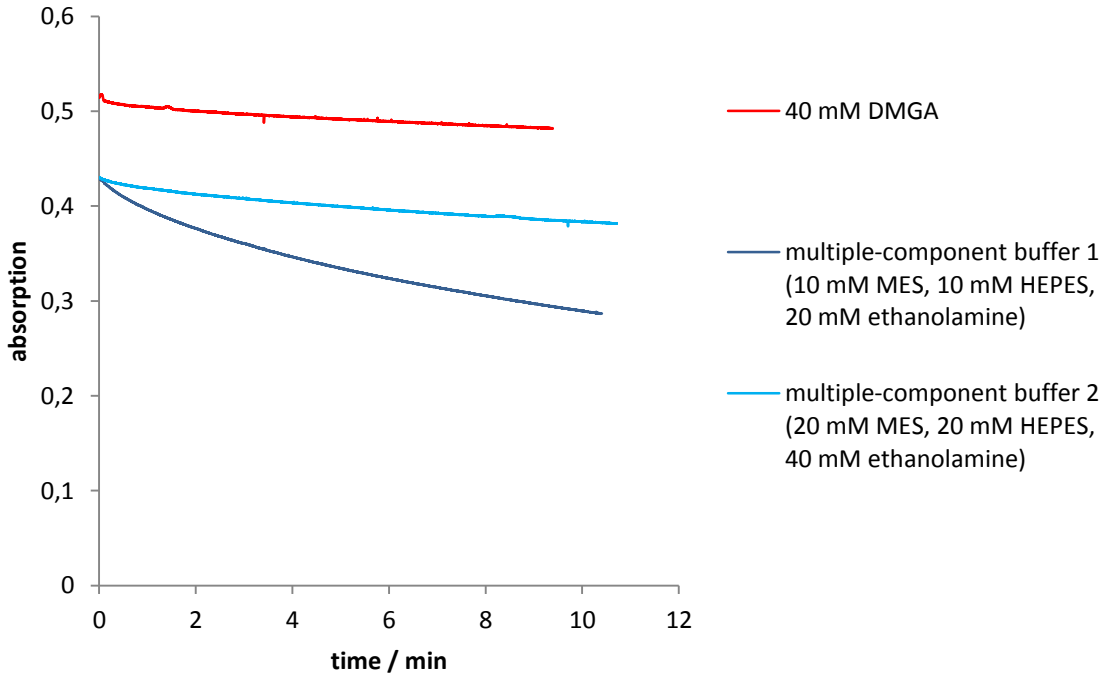

Figure 4-6 **Continuous photometrical measurement of the decrease of the concentration of quinonediimine dye in different buffer conditions**

For all three buffers a decrease of absorption is observed, which leads to the assumption that the formed quinonediimine dye is not completely stable over time. This instability seems to be buffer-dependent as it is negligible with 40 mM DMGA and multiple-component buffer 2, but significant for multiple-component buffer 1. The initial absorption measured for the enzymatic assay reaction in 40 mM DMGA is higher than for both multiple-component buffers.

Resume

According to the present results it was decided to use the continuous enzymatic assay for the measurements for the entire pH profile for the wild type and LOX mutant Y215F, as described in section 2.4.2. Instead of 40 mM DMGA multiple-component buffer 2 from pH 5 to pH 10 was used for all measurements. The resulting specific activity is lower in multiple-component buffer 2 compared to DMGA and probably as the actual activity. But as the resulting values at different pH values are comparable among themselves, multiple-component buffer 2 was considered as adequate buffer for compiling pH studies.

4.2.pH studies for the wild type and Y215F mutant

4.2.1. Material and methods

4.2.1.1. Determination of enzyme kinetics

10 µL LOX version appropriately diluted in 50 mM potassium phosphate buffer or H_2O was added to a coupled assay solution containing multiple-component buffer 2 (20 mM MES, 20 mM HEPES and 40 mM ethanolamine) at various pH values (pH 5 – 10), 10 units peroxidase, 1.5 mM 4-aminoantipyrine, 0.04 v/v% N,N-dimethylaniline and L-lactate (up to ten various concentrations for compiling Michaelis-Menten kinetic) in a total volume of 0.5 mL reaction mixture. After reaction time of 10 minutes at 37 °C 1 mL 0.25 w/v % dedecylbenzenesulfonic acid solution was added to stop the reaction. The absorbance was measured spectrophotometrically at 565 nm with a Varian Cary® 50 Bio UV-Visible Spectrophotometer at RT directly after addition of DBS. Specific activity was calculated with Equation 2-1 and Equation 2-2.

4.2.1.2. Data analysis

Determination of respective kinetic data k_{cat} and K_M at different pH values for the Y215F mutant and the wild type occurred via SigmaPlot® (version 11.0) and by using Equation 2-3, Equation 2-4 and Equation 2-5.

The pH profiles of log(k_{cat}) and log(k_{cat}/K_M) were non-linear fitted to Equation 4-1. This equation was used because of curve characteristics, i.e. a “bell-shaped” curve with two observed pK values.

$$logY = \log\left[\frac{C}{1+\frac{[H^+]}{K_1}+\frac{K_2}{[H^+]}}\right] \qquad \textbf{Equation 4-1}$$

where Y is k_{cat} or k_{cat}/K_M, C is the pH independent value of Y at the optimal state of protonation, $[H^+]$ is the proton concentration and K_1 and K_2 are macroscopic dissociation constants (Greene et al. 1992, Schwarz et al. 2007, Klimacek et al. 2010).

4.2.1. Results

pH profiles of k_{cat} and k_{cat}/K_M were determined for the Y215F mutant and the wild type and are shown in Table 4-6 and Table 4-7 and in double-log plots (see Figure 4-7 – Figure 4-9).

Table 4-6 Kinetic data of Y215F at different pH values

pH	Specific activity / U/mg	k_{cat} / s^{-1}	K_M / mM	k_{cat}/K_M / $s^{-1}mM^{-1}$	K_{IS} / mM
5.0	11.0 ± 1.4	7.55 ± 0.38	1.30 ± 0.31	5.79	-
5.5	17.0 ± 0.7	11.6 ± 0.2	0.12 ± 0.01	95.4	587 ± 250
6.0	27.0 ± 1.8	18.5 ± 0.5	0.06 ± 0.01	301	454 ± 244
6.5	52.9 ± 1.4	36.1 ± 1.0	0.07 ± 0.01	695	210 ± 52
7.0	34.7 ± 2.3	23.7 ± 0.6	0.09 ± 0.01	252	78.4 ± 12.3
7.5	22.4 ± 0.8	15.3 ± 0.2	0.07 ± 0.00	224	94.4 ± 9.5
8.0	4.22 ± 0.19	2.88 ± 0.05	0.02 ± 0.01	134	316 ± 88
8.5	2.09 ± 0.07	1.43 ± 0.02	0.04 ± 0.00	33.0	471 ± 129
9.0	0.37 ± 0.02	0.26 ± 0.01	0.13 ± 0.10	1.94	-
9.5	0.04 ± 0.03	0.03 ± 0.01	5.45 ± 2.62	0.01	38.2 ± 19.8
10.0	0.15 ± 0.03	0.10 ± 0.01	1.13 ± 0.28	0.09	46.4 ± 11.8

Table 4-7 Kinetic data of the wild type at different pH values

pH	Specific activity / U/mg	k_{cat} / s^{-1}	K_M / mM	k_{cat}/K_M / $s^{-1}mM^{-1}$	K_{IS} / mM
5.0	82.7 ± 3.9	56.5 ± 2.6	13.9 ± 1.7	4.07	-
5.5	112 ± 10	76.8 ± 6.9	13.1 ± 3.7	5.88	-
6.0	169 ± 5	116 ± 3	1.89 ± 0.26	61.3	-
6.5	287 ± 8	196 ± 6	0.89 ± 0.13	221	-
7.0	350 ± 7	239 ± 5	0.99 ± 0.06	241	-
7.5	223 ± 3	153 ± 2	0.81 ± 0.03	189	-
8.0	197 ± 5	135 ± 3	0.61 ± 0.04	222	-
8.5	101 ± 2	69.3 ± 1.7	1.24 ± 0.11	55.8	-
9.0	50.9 ± 5.2	34.8 ± 3.6	0.57 ± 0.20	61.6	253 ± 264
9.5	13.1 ± 0.8	8.94 ± 0.53	0.67 ± 0.14	13.3	278 ± 177
10.0	1.26 ± 0.27	0.86 ± 0.18	9.35 ± 3.12	0.10	28.5 ± 11.0

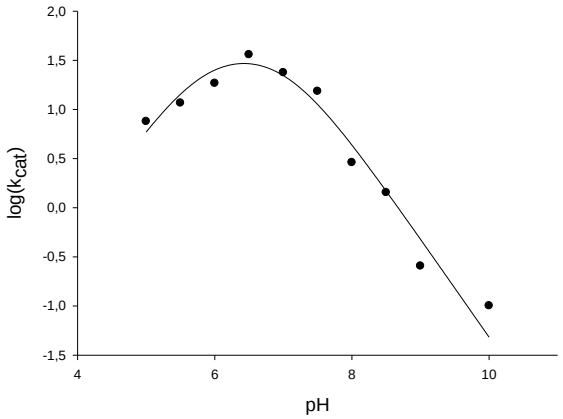

Figure 4-7 **pH dependence of k_{cat} in Y215F**

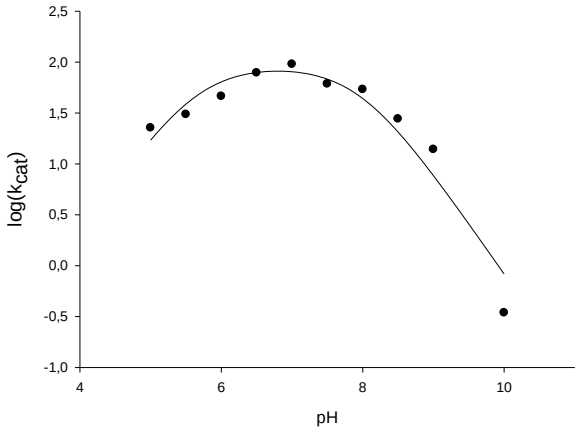

Figure 4-8 **pH dependence of k_{cat} in the wild type**

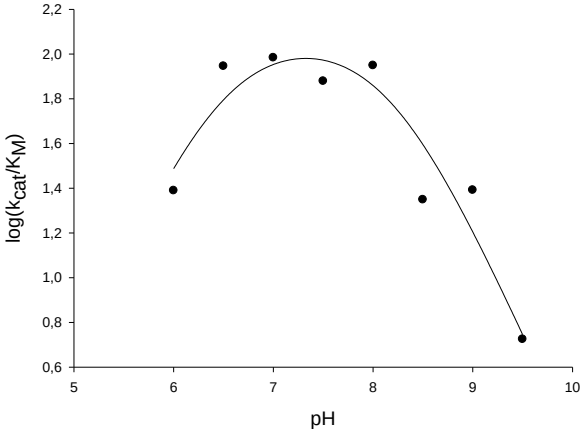

Figure 4-9 pH dependence of k_{cat}/K_M in the wild type

Table 4-8 **Apparent pK values in Y215F and the wild type**

Mutant/wild type	Parameter	pK_1	pK_2	C	R^2
wild type	$\log(k_{cat})$	5.65	7.95	90.9 s^{-1}	0.97
	$\log(k_{cat}/K_M)$	6.47	8.18	123 $mM^{-1}s^{-1}$	0.95
Y215F	$\log(k_{cat})$	5.80	7.05	43.4 s^{-1}	0.98
	$\log(k_{cat}/K_M)$	n.d.	n.d.	n.d.	0.87

As seen in the figures above and Table 4-8 the wild type and Y215F mutant have two pK values. pK_1 shows the requirement for a group to be unprotonated for optimum enzyme activity and pK_2 shows the requirement for a group to be protonated. The "bell-shaped" curve of $\log(k_{cat})$ versus pH for the wild type is well fitted and results in a pK_1 of 5.65 and pK_2 of 7.95, thus two ionizable groups are

visible. Log (k_{cat}/K_M) versus pH has a low R^2 and results in a pK_1 of 6.47, which differs significant from the resulting pK_1 of log(k_{cat}) versus pH, and a pK_2 of 8.18, which is similar to the pK_2 resulting from log(k_{cat}) versus pH. These results lead to the assumption, that pK_1 is K_M-dependent whereas pK_2 not. It is not exactly known, not even in literature, which active site residues lead to the determined pK values. pK_1 could derive from His^{265}. The imidazol ring of histidine has under physiological conditions a pK of about 6 (Wallace Cleland 1982).

For the Y215F the apparent pK values resulting from log(k_{cat}) versus pH are 5.80 for pK_1 and 7.05 for pK_2. Thus a remarkable change of the pK values due to mutation at Tyr^{215} is only observed for pK_2. pK_2 in Y215F is lowered by one pH unit compared to the wild type. As the influence of the active site residues on the pK of the enzyme is not exactly understood, only assumptions to the change of pK_2 in Y215F can be made. Tyrosine has a pK of 10 under physiological conditions. It could influence the pK of other active site residues, the pK_2 respectively. Thus the removal of tyrosine in Y215F might cause the lowered pK_2 (Wallace Cleland 1982).

The curve resulting of log(k_{cat}/K_M) versus pH could not be fitted well and thus results cannot be used for comparison with data of Table 4-8.

An influence of the substrate on the pK values can be excluded. L-lactate has a pK of 3.9 and in this pH range no kinetic measurements were conducted.

5. Discussion

The active site LOX mutants Y215F and Y215H had influences on kinetic parameters of the enzyme. There is a decrease of specific activity for L-lactate observed for both mutants compared to the wild type. This decrease might occur from the involvement of the Tyr^{215} residue in stabilization processes in the active site in the wild type, due to the Tyr^{215} hydroxyl group, which is missing in Y215F and Y215H. Furthermore the low activity of Y215H might result from the change in steric properties in the active site compared to the wild type. It is remarkable that there still exists an activity of the LOX mutants, which confirms the assumption, that Tyr^{215} is not directly involved in substrate conversion. Though it could play a role in substrate binding and stabilization.

Substrate specificity did not change significantly due to mutations. There is a slight decrease, or increase respectively, of the Michaelis constant for glycolic acid for Y215F and Y215H. In addition there is a negligible change in kinetic data for long chain, branched and linear, L-α-hydroxy acids.

In literature several methods are mentioned (see Sobrado, 2003) to find out more about the mechanism of L-α-hydroxy acids and the involvement of active site residues. One of these opportunities was conducted, namely pH studies. Kinetic data at different pH values for Y215F mutant and the wild type were compared (see section 4.2). There is a slight difference between the pK values of the mutant and the wild type in the basic range. This could bring out that the residue at position 215 in the enzyme influences active site residues, which are involved in substrate binding or conversion. Probably the residue itself is not involved in protonation or deprotonation of the substrate or the cofactor FMN. The lowered pK_2 in Y215F might result from the mutation. Tyrosine has a pK of 10 and might influence the pK values of other active site residues. In Y215F tyrosine is replaced by phenylalanine and therefore the pK value of the enzyme is changed due to the missing influence of the tyrosine.

There is no remarkable change of the pK in the acid range of the profile for the mutant compared to the wild type. pK_1 in Y215F and the wild type is approximately 6. The crucial residue might be His^{265}.

At different pH values substrate inhibition in the wild type, as well as in Y215F, could be observed (see Table 4-6 and Table 4-7). Apart from pH 5.0 and pH 9.0 substrate inhibition is observed in Y215F at every determined pH value. The mentioned exceptions could result either from measuring and sampling inaccuracy or it could describe the phenomenon that at pH 5.0 and pH 9.0 no second substrate binding site, which further leads to substrate inhibition, is found. As in the wild type substrate inhibition at pH 9.0 is observed, it can be assumed that phenylalanine avoids substrate inhibition in Y215F at pH 9.0. In the wild type substrate inhibition occurs in the basic range from

pH 9.0 to pH 10.0. This might result from deprotonation of the tyrosine, which would mean that Tyr^{215} has a pK lower than 9.0. That would coincide with the assumptions made above based on the pH studies, where Tyr^{215} influences the pK of the enzyme in the basic range.

To find out more about the observed influences of Tyr^{215} further experiments and analyzes are necessary. First of all comparison with pH studies of the Y215H mutant could be reasonable. Furthermore stopped-flow measurements at significant pH values could give more information about the influence of the residue in reductive and oxidative half-reaction. Last but not least the determination of isotope effects by D-lactate is planned and going to be conducted in the near future.

6. Tables

6.1. References

Bisswanger, H. 2002. Substrate inhibition. *Enzyme kinetics - principles and methods.* Weinheim : Wiley-VCH Verlag GmbH, 2002, pp. 120-121.

Corbett, J.F. 1969. Benzoquinone imines. Part II. Hydrolysis of p-benzoquinone monoimine and p-benzoquinone diimine. *Journal of the Chemical Society B.* 1969, pp. 213-216.

Dubois, J., Chapman, S.K., Mathews, F.S., Reid, G.A. and Lederer, F. 1990. Substitution of Tyr^{254} with Phe at the active site of flavocytochrome b_2: consequences on catalysis of lactate dehydrogenation. *Biochemistry.* 29, 1990, pp. 6393-6400.

Ellis, K.J. and Morrision, J.F. 1982. Buffers of constant ionic strength for studying pH-dependent processes. *Methods in Enzymology.* 87, 1982, pp. 405-425.

Fitzpatrick, P.F. 2001. Substrate dehydrogenation by flavoproteins. *Accounts of Chemical Research.* 34 (4), 2001, pp. 299-307.

Fox, M.A. and Whitesell, J.K. 1995. Thiaminpyrophosphat: Decarboxylierung von α-Ketosäuren. *Organische Chemie.* Heidelberg-Berlin-Oxford : Spektrum Akademischer Verlag, 1995, pp. 783-787.

Frebel, H., Chemnitius, G.C., Cammann, K., Kakerow, R., Rospert, M. and Mokwa, W. 1997. Multianalyte sensor for the simultaneous determination of glucose, L-lactate and uric acid based on microelectrode arry. *Sensors and Actuators B: Chemical.* 43, 1997, pp. 87-93.

Furuichi, M., Suzuki, N., Dhakshnamoorhty, B., Minagawa, H., Yamagishi, R., Watanabe, Y., Goto, Y., Kaneko, H., Yoshida, Y., Yagi, H., Waga, I., Kumar, P.K.R. and Mizuno, H. 2008. X-ray structures of *Aerococcus viridans* lactate oxidase and its complex with D-lactate at pH 4.5 show an α-hydroxyacid oxidation mechanism. *Journal of Molecular Biology.* 378, 2008, pp. 436-446.

Greene, D., Das, B. and Fricker, L.D. 1992. Regulation of carboxypeptidase E: effect of pH, temperature and Co^{2+} on kinetic parameters and substrate hydrolysis. *Biochemical Journal.* 285, 1992, pp. 613-618.

Klimacek, M. and Nidetzky, B. 2010. The oxyanion hole of *Pseudomonas fluorescens* mannitol 2-dehydrogenase: a novel structural motif of electrostatic stabilization in alcohol dehydrogenase active sites. *Biochemical Journal.* 425, 2010, pp. 455-463.

Leiros, I., Wang, E., Rasmussen, T., Oksanen, E., Repo, H., Petersen, S.B., Heikinheimo, P. and Hough, E. 2006. The 2.1 Å structure of *Aerococcus viridians* L-lactate oxidase (LOX). *Acta Crystallographica Section F Structural Biology and Crystallization Communications.* 62, 2006, pp. 1185-1190.

Maeda-Yorita, K., Aki, K., Sagai, H., Misaki, H. and Massey, V. 1995. L-lactate oxidase and L-lactate monooxygenase: Mechanistic variations on a common structural theme. *Biochimie.* 77, 1995, pp. 631-642.

Pernet, P., Bénéteau-Burnat, B., Vaubourdolle, M., Maury, E. and Offenstadt, G. 2009. False elevation of blood lactate reveals ethylene glycole poisoning. *American Journal of Emergency Medicine.* 27, 2009, pp. 132.e1-132.e2.

Schwarz, A., Brecker, L. and Nidetzky, B. 2007. Acid base catalysis in *Leuconostoc mesenteroides* sucrose phophorylase probed by site-directed mutagenesis and detailed kinetic comparison of wild-type and Glu^{237} --> Gln mutant enzymes. *Biochemical Journal.* 403, 2007, pp. 441-449.

Sobrado, P. and Fitzpatrick, P.F. 2003. Solvent and primary deuterium isotope effects show that lactate CH and OH bond cleavages are concerted in Y254F flavocytochrome b_2, consistent with a hydride transfer mechanism. *Biochemistry.* 42, 2003, pp. 15208-15214.

Streitenberger, S.A., López-Mas, J.A., Sánchez-Ferrer, Á. and García-Carmona, F. 2001. Non-linear slow-binding inhibition of *Aerococcus viridans* lactate oxidase by Cibacron Blue 3GA. *Journal Enzyme Inhibition.* 16 (4), 2001, pp. 301-312.

Umena, Y., Yorita, K., Matsuoka, T., Kita, A., Fukui, K. and Morimoto, Y. 2006. The crystal structure of L-lactate oxidase from *Aerococcus viridans* at 2.1 Å resolution reveals the mechanism of strict substrate recognition. *Biochemical and Biophysical Research Communications.* 350 (2), 2006, pp. 249-256.

Wallace Cleland, W. 1982. The use of pH studies fo determine chemical mechanisms of enzyme-catalyzed reactions. *Methods in Enzymology.* 87, 1982, pp. 390-405.

Wang, W. and Malcolm, B.A. 1999. Two stage PCR protocol allowing introduction of multiple mutations, deletions and insertions using QuikChange Site-Directed Mutagenesis. *Biotechniques.* 26, 1999, pp. 680-682.

Yorita, K., Aki, K., Ohkuma-Soyejima, T., Kokubo, T., Misaki, H. and Massey, V. 1996. Conversion of L-lactate oxidase to a long chain α-hydroxy acid oxidase by site-directed mutagenesis of alanine 95 to glycine. *The journal of biological chemistry.* 271 (45), 1996, pp. 28300-28305.

6.2.Abbreviations

Abbreviation	Explanation
4-AAP	4-aminoantipyrine
AEC	anionic exchange chromatography
ADH	alcohol dehydrogenase
amp	ampicillin
bp	base pair
BSA	bovine serum albumin
c	concentration
CIP	cleaning in place
CV	column volume
Da	Dalton
DBS	dodecylbenzenesulfonic acid
DMA	N,N-dimethylaniline solution
DMGA	3,3-dimethylglutaric acid
dNTP	deoxyribonucleotide triphosphate
E. coli	*Escherichia coli*
EDTA	ethylenediaminetetraacetic acid
e.g.	for example
EtBr	ethidium bromide
F	phenylalanine
ferm	protein expression by fermentation
FMN	flavomononucleotide
fw	forward
H	histidine
HIC	hydrophobic interaction chromatography
His	histidine
i.e.	id est (that is)
IPTG	isopropyl-β-D-thiogalactopyranoside
k_{cat}	turnover number
k_{cat}/K_M	catalytic efficiency
K_I	dissociation constant of enzyme-inhibitor complex
K_{IS}	dissociation constant of enzyme-inhibitor-substrate complex
K_M	Michaelis constant

Abbreviation	Explanation
L	liter
LB	lysogeny broth
LMO	L-lactate monooxygenase
LMW	low molecular weight
LOX	L-lactate oxidase
m	meter
M	molar
$MgCl_2$	magnesium(II)-chloride
min	minute
NaCl	sodium chloride
n.d.	non detectable
NLT	not lower than
NMT	not more than
OD	optical density
onc	overnight culture
pO_2	partial pressure of oxygen
POD	peroxidase
rev	reverse
rpm	rotations per minute
RT	room temperature
TAE	Tris-acetate-EDTA
Tyr	tyrosine
UV	ultraviolet
v/v	volume per volume
WT	wild type
w/v	weight per volume
w/w	weight per weight
Y	tyrosine

6.3.Buffers, media and solutions

All buffers, media and solutions prepared are listed in the following table. All reagents were, if not mentioned, supplied either by Sigma Aldrich Corp. or Carl Roth GmbH + Co KG.

Buffer/Medium/Solution	**Composition**
1 % agarose gel	10 g agarose/L in 1 mM TAE buffer, dissolved at 100 °C and addition of 15 µL/50 mL EtBr after gel preparation minimum 20 min. drying time
Ammonium sulfate 1.5 M in potassium phosphate buffer, pH 7.0	198.2 g/L in potassium phosphate buffer 50 mM, pH 7.0, pH adjusted with NaOH and HCl, sterile-filtered 0.2 µm
Ammonium sulfate 3 M, pH 7.0	396.4 g/L in potassium phosphate buffer 50 mM, pH 7.0, pH adjusted with NaOH and HCl, sterile-filtered 0.2 µm
Ampicillin stock 1000x	115 mg/mL ampicillin in H_2O, sterile-filtered 2 µm
BisTris 50 mM, pH 5-7	10.46 g/L in H_2O, pH adjusted with NaOH and HCl, sterile-filtered 0.2 µm
Destain solution (SDS-PAGE)	30 % ethanol and 10 % acetic acid in H_2O
Dying solution (SDS-PAGE)	PhastGel^{TM} Blue R Coomassie R350 (GE Healthcare Life Sciences) stock and 20 % acetic acid 1 : 1 (v/v)
Ethanolamine 50 mM, pH 8.5-10	3.05 g/L in H_2O, pH adjusted with NaOH and HCl, sterile-filtered 0.2 µm
Fermentation medium A	starter culture: 5.5 g/L glucose in H_2O main culture: 20 g/L glucose in H_2O (concentrations correspond to final concentration after combination with fermentation medium B and C)
Fermentation medium B	starter/main culture: 10 g/L peptone, 5 g/L yeast extract, 5 g/L NaCl, 1 g/L NH_4Cl, 0.25 g/L $MgSO_4$ * 7 H_2O, 1 mL/L trace element solution and 100 µL/L polypropylene glycol in H_2O (concentrations correspond to final concentration after combination with fermentation medium A and C)
Fermentation medium C	starter/main culture:

Buffer/Medium/Solution	Composition
	3 g/L K_2HPO_4 and 6 g/L KH_2PO_4 in H_2O (concentrations correspond to final concentration after combination with fermentation medium A and B)
further Fermentation solutions	• 2M (112 g/L) KOH • 1M (98 g/L) H_3PO_4 • 2 mg/mL thiamine, sterile-filtered 0.2 µm • 100 mg/mL ampicillin, sterile-filtered 0.2 µm
Glycerol 30%	30 w/w% glycerol in H_2O, autoclaved
Glycolic acid 200 mM, pH 6.5	15.21 g/L in H_2O, pH adjusted with NaOH
HEPES 150 mM, pH 7-8.5	35.75 g/L in H_2O, pH adjusted with NaOH and HCl, sterile-filtered 0.2 µm
IPTG 1000x	250 µg/mL dissolved in H_2O, sterile-filtered 0.2 µm
LB medium	10 g/l peptone, 5 g/L NaCl and 5 g/L yeast extract in H_2O, autoclaved
LB-amp medium	LB medium, autoclaved, with 1 µL 1000x ampicillin stock in H_2O (sterile-filtered 0.2 µm) / mL medium
LB-amp plates	LB medium with 18 g/L agar, autoclaved and 1 µL 1000x ampicillin stock in H_2O (sterile-filtered 0.2 µm) / mL medium added
L-2-hydroxybutyric acid 200 mM, pH 6.5	20.82 g/L in H_2O, pH adjusted with NaOH
L-2-hydroxyisocaproic acid 400 mM, pH 6.5	52.86 g/L in H_2O, pH adjusted with NaOH
L-2-hydroxy-3-methylbutyric acid 200 mM, pH 6.5	23.63 g/L in H_2O, pH adjusted with NaOH
L-lactic acid 50 mM, pH 6.5	4.50 g/L in H_2O, pH adjusted with NaOH
L-mandelic acid 200 mM, pH 6.5	30.43 g/L in H_2O, pH adjusted with NaOH
Multiple component buffer 1, pH 5-10	50 mM (9.76 g/L) MES, 50 mM (23.83 g/L) HEPES and 100 mM (12.22 g/L) ethanolamine in H_2O, pH adjusted with NaOH and HCl, defined ionic strength adjusted with NaCl, sterile-filtered 0.2 µm
Multiple component buffer 2, pH 5-10	100 mM (19.52 g/L) MES, 100 mM (11.92 g/L) HEPES and 200 mM (6.11 g/L) ethanolamine in H_2O,

Buffer/Medium/Solution	Composition
	pH adjusted with NaOH and HCl, defined ionic strength adjusted with NaCl, sterile-filtered 0.2 µm
Potassium chloride 2 M	149.1 g/L KCl in H_2O, sterile-filtered 0.2 µm
Potassium chloride 1 M in potassium phosphate buffer, pH 7.0	76 g/L KCl in 50 mM potassium phosphate buffer, pH adjusted with NaOH , sterile-filtered 0.2 µm
Potassium phosphate 50 mM, pH 7.0	50 mM (6.8 g/L) KH_2PO_4 (in H_2O) and 50 mM (13.1 g/L) K_2HPO_4 (in H_2O) were merged at the ratio of 1 : 1.4, pH adjusted with NaOH and HCl, sterile-filtered 0.2 µm
Preserve solution (SDS-PAGE)	10 % acetic acid and 13 % glycerol in H_2O
SOC medium	20 g/L peptone, 0.58 g/L NaCl, 5 g/L yeast extract, 0.18 g/L KCl, 2.04 g/L $MgCl_2$ and 2.46 g/L $MgSO_4$ in H_2O after autoclavation adding of 3.60 g/L glucose
Sodium hydroxide 1M / 0.5 M	40.2 g/L /20.1 g/L NaOH in H_2O, sterile-filtered 0.2 µm
TAE buffer 1 mM	40 mM (4.85 g/L) Tris pH 8.3, 40 mM (2.40 g/L) acetate and 1 mM (0.29 g/L) EDTA in H_2O
Trace elements solution (fermentation)	4 g/L $FeSO_4$*7 H_2O, 1 g/L $MnSO_4$*H_2O, 0.4 g/L $CoCl_2$, 0.15 g/L $CuSO_4$*5 H_2O, 0.1 g/L H_3BO_3, 0.2 g/L $ZnSO_4$*7 H_2O, 0.2 g/L Na_2MoO_4*2 H_2O and 0.4 g/L $FeCl_3$ dissolved in 5 M HCl

6.4.Tables

6.5.Figures

Appendix

Supplemental methods and figures

Site-directed mutagenesis

The vector supplied by Roche Diagnostics is shown in Figure A. Its size is 4062 bp. Important features are marked, such as the *tac* promoter, ORF for LOX WT and ampicillin residence.

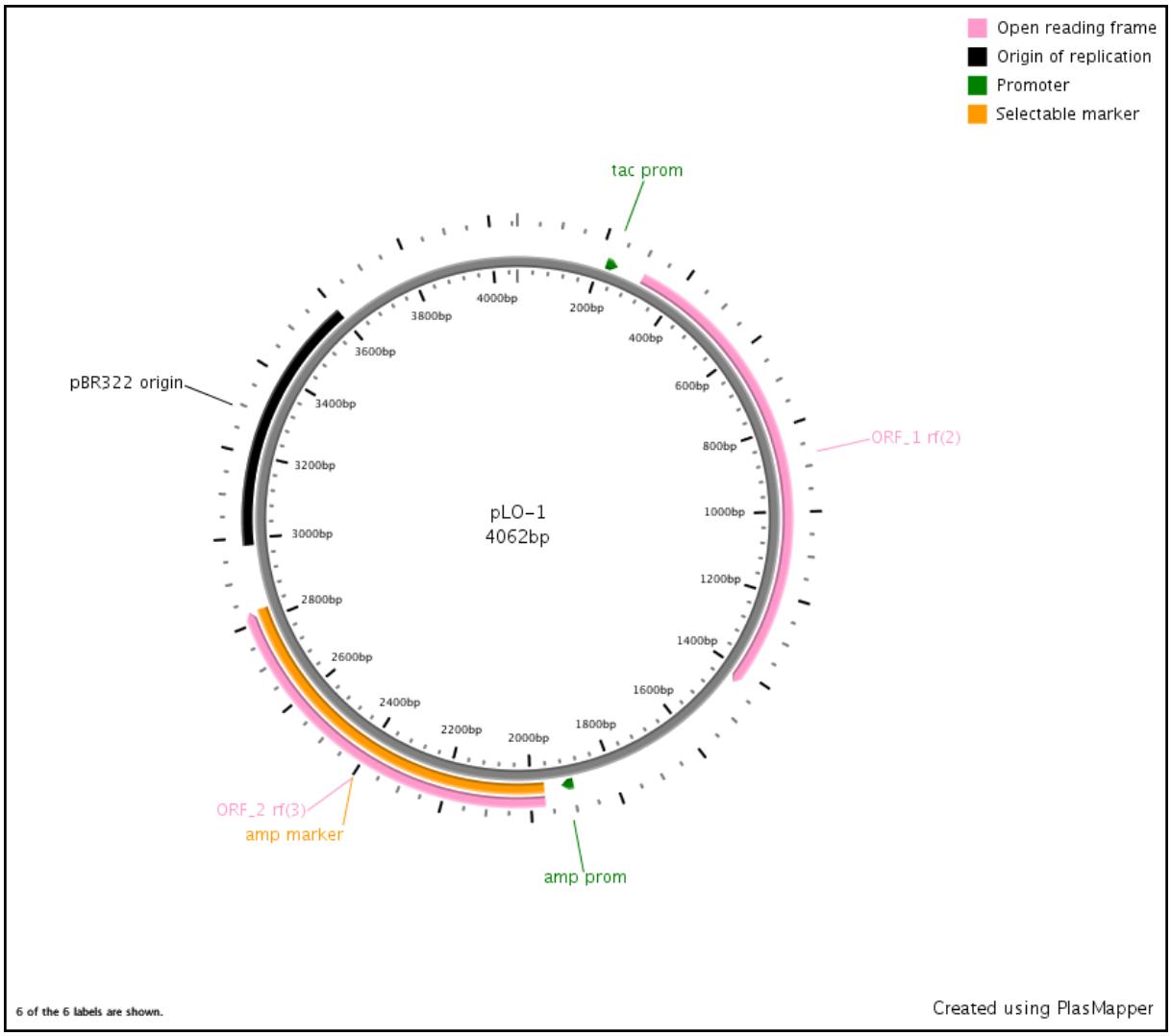

Figure A **pLO-1 vector with significant features**

As strain for protein expression *E. coli* BL21 (DE3), with the chromosomal genotype *E. coli* B dcm ompT hsdS($r_B^-m_B^-$) gal, was used.

Figure B shows lanes and the correspondent DNA fragment size of GeneRuler™ 100 bp Plus DNA Ladder from Fermentas.

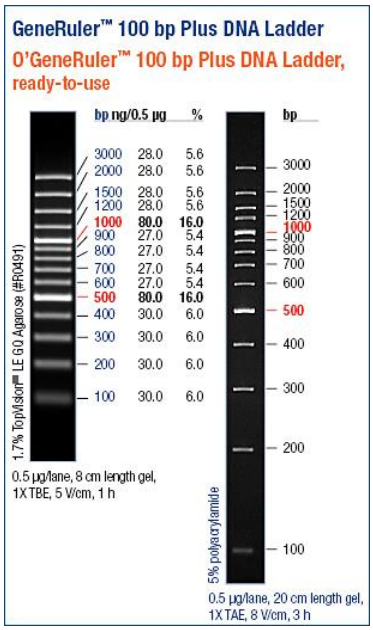

Figure B **GeneRuler™ 100 bp Plus DNA Ladder (Fermentas)**

In Table A the sequence of the primer used for sequencing of the supposed LOX mutants (Integrated DNA Technologies Inc.) is mentioned.

Table A **Primer for DNA sequencing of supposed LOX mutants**

Primer	Sequence	T_m / °C
SeqLOX1fw	5'-GCAAGATGTTGAAGCGCCTGATAC-3'	58.6

Colony PCR

Colony PCR was used to screen for successful mutagenesis as well as successful transformation directly from *E. coli* colonies. Cells were resuspended in 20 µL H_2O and incubated at 95 °C for 10 minutes. For the Colony PCR 2 µL of the resuspended cells were merged with 5 pM of each primer (fw and rev), 2 µL 10 x *Taq* buffer (Fermentas), 200 µM dNTPs (Fermentas), 1.25 mM $MgCl_2$ and 0.06 U *Taq* polymerase (Fermentas) on ice. Denaturation occurred at 95 °C for 2 minutes, followed by 30 cycles, each containing of 15 seconds at 95 °C, 30 seconds at 55 °C and 60 seconds at 72 °C. Final elongation occurred at 72 °C of 2 minutes. After digestion with *NheI* 6 x DNA Loading dye (Fermentas) was added to the cool-down PCR mixture to perform agarose gel-electrophoresis and to verify if mutagenesis as well as transformation was successful.

Purification

Figure C shows exemplarily a chromatogram of a HIC run, realized with Y215H.

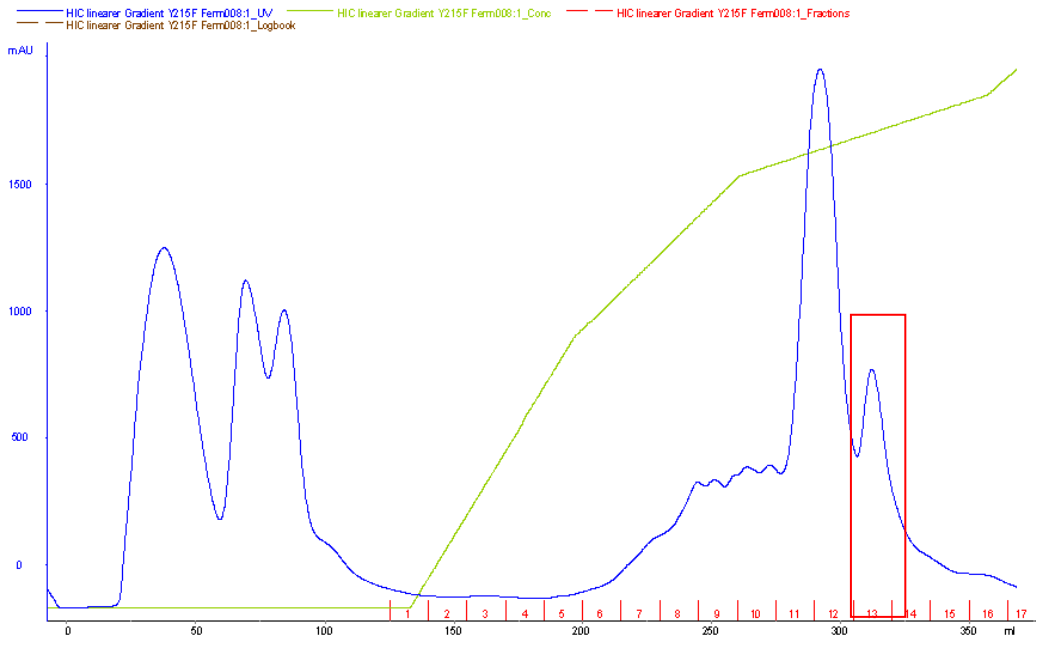

Figure C **HIC purification run with linear gradient of Y215H, LOX mutant was found in highlighted peak**

Figure D shows a chromatogram of an AEC run, realized with LOX mutant Y215H.

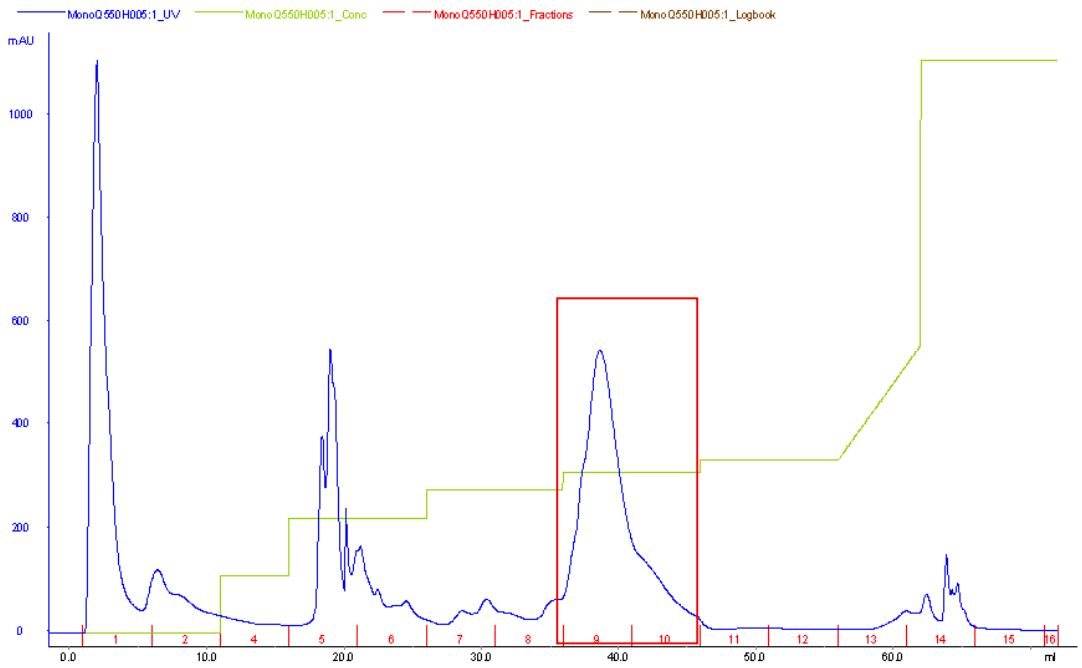

Figure D **AEC purification run mutant with stepwise gradient of Y215H, LOX mutant was found in highlighted peak**

SDS-PAGE

Figure E shows the used low molecular weight marker (GE Healthcare) for SDS-PAGE and the size of the corresponding protein.

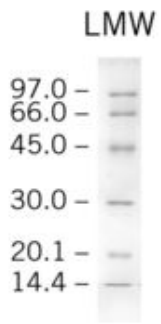

Figure E **Low molecular weight marker (GE Healthcare)**

Supplemental results and figures of pH studies

Michaelis-Menten plots

Following figures show Michaelis-Menten plots (enzyme activity versus substrate concentration) for the wild type and Y215F mutant at pH 5-10 with L-lactate as substrate.

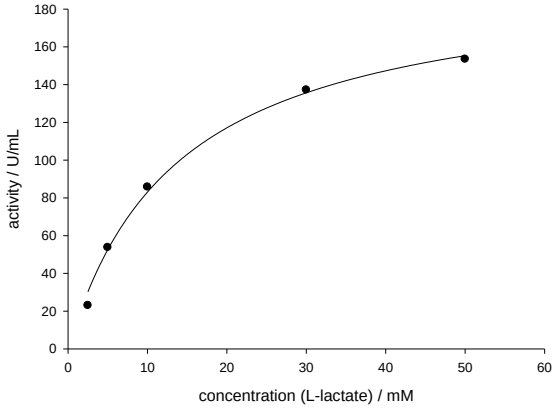

Figure F **Wild type at pH 5.0**

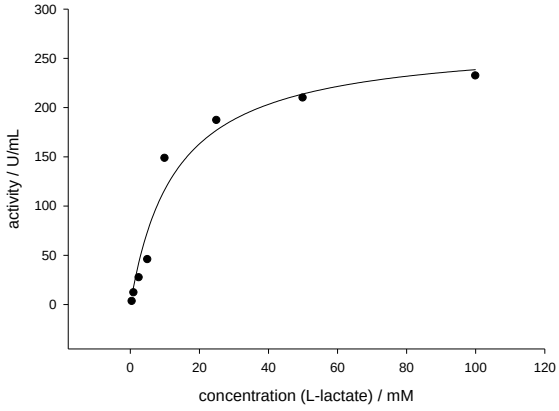

Figure G **Wild type at pH 5.5**

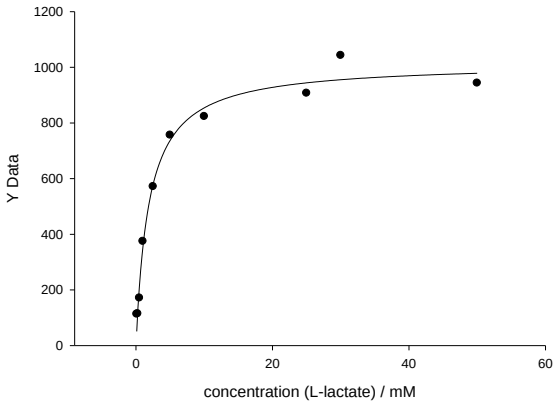

Figure H **Wild type pH at 6.0**

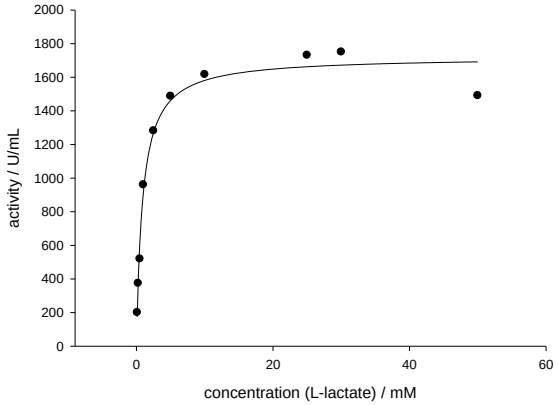

Figure I **Wild type at pH 6.5**

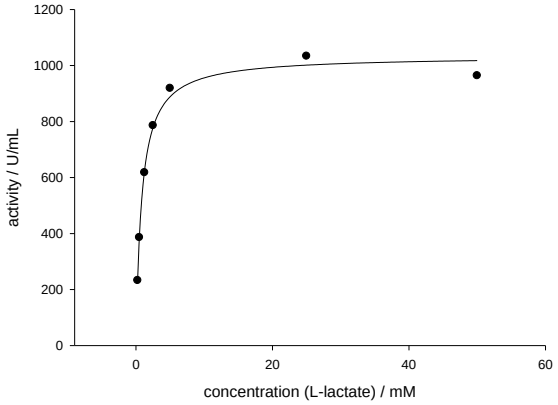

Figure J **Wild type at pH 7.0**

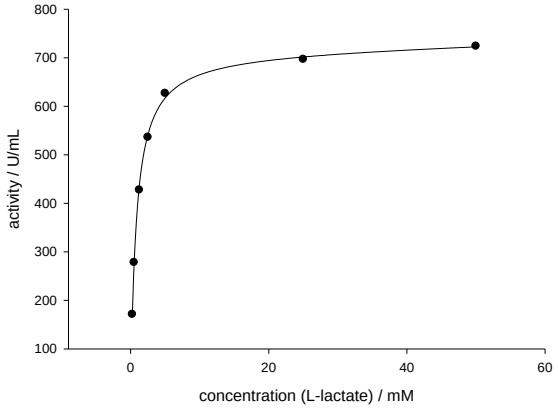

Figure K **Wild type at pH 7.5**

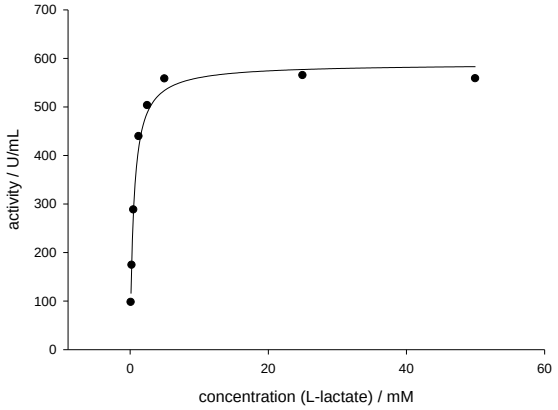

Figure L **Wild type at pH 8.0**

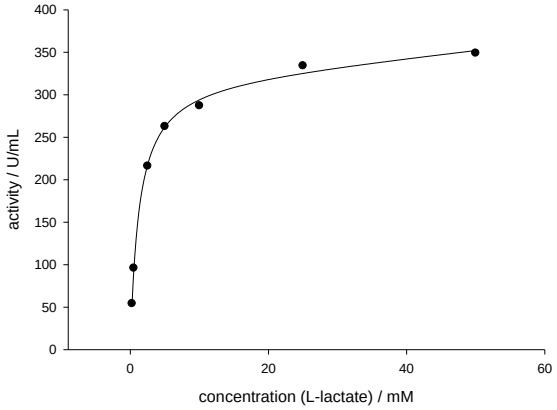

Figure M **Wild type at pH 8.5**

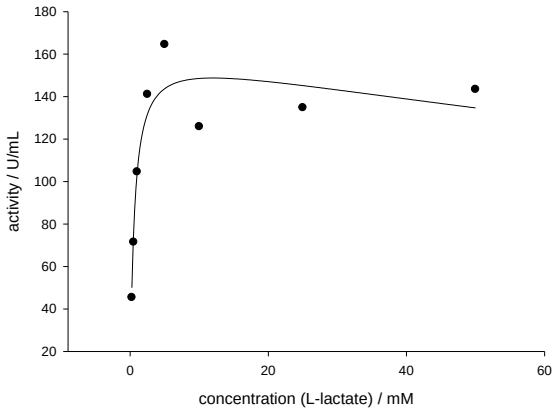

Figure N **Wild type at pH 9.0**

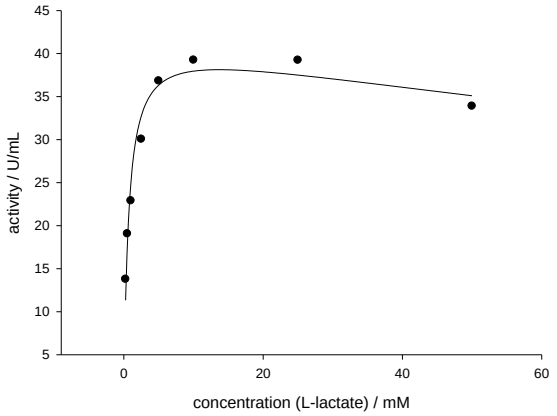

Figure O **Wild type at pH 9.5**

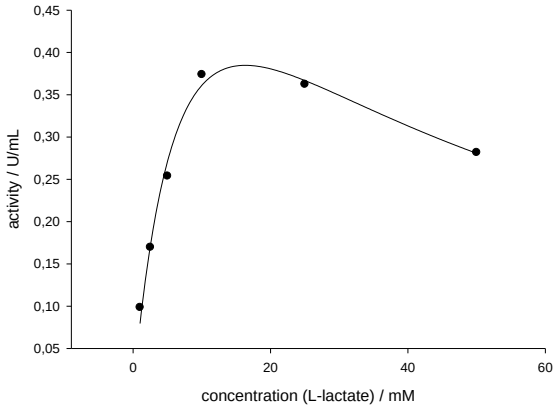

Figure P **Wild type at pH 10.0**

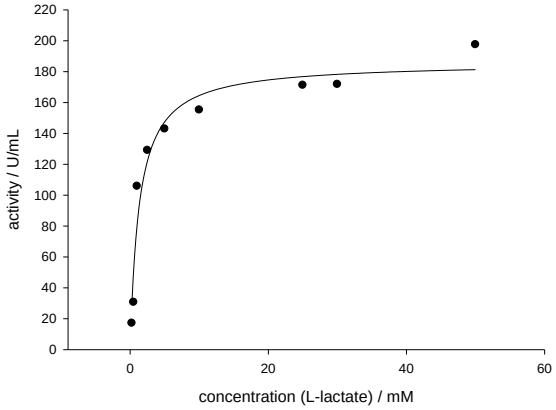

Figure Q **Y215F at pH 5.0**

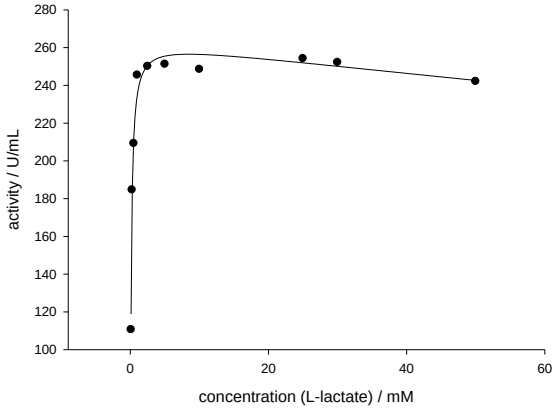

Figure R **Y215F at pH 5.5**

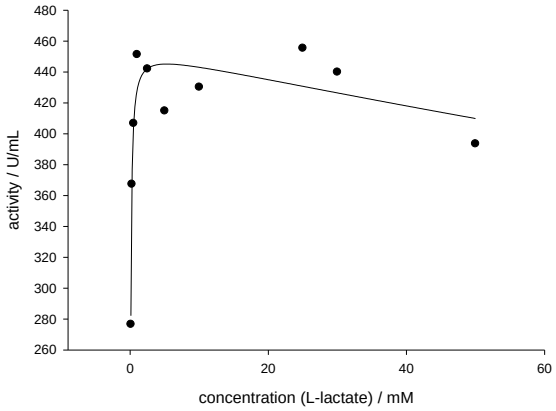

Figure S **Y215F at pH 6.0**

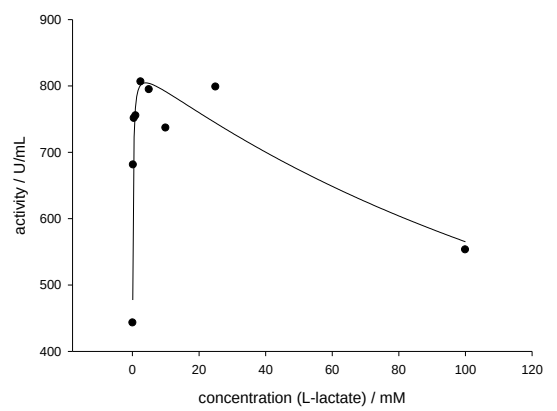

Figure T **Y215F at pH 6.5**

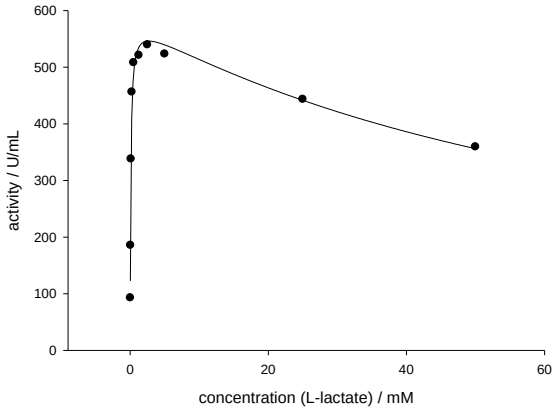

Figure U **Y215F at pH7.0**

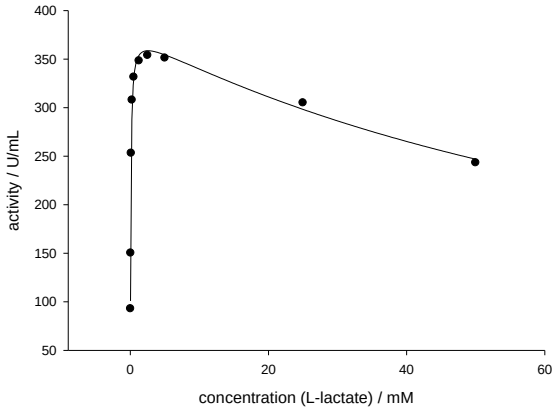

Figure V **Y215F at pH7.5**

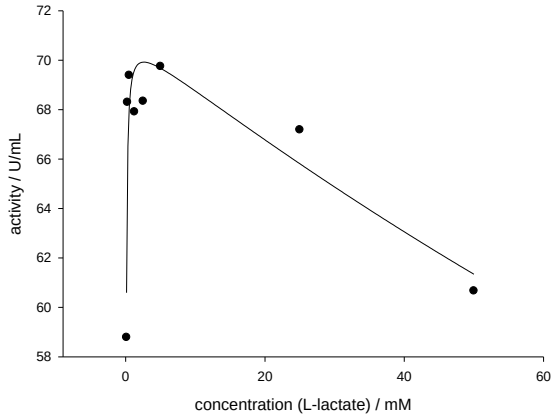

Figure W **Y215F at pH8.0**

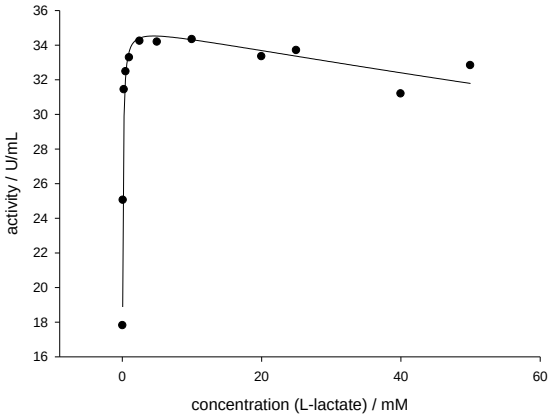

Figure X **Y215F at pH8.5**

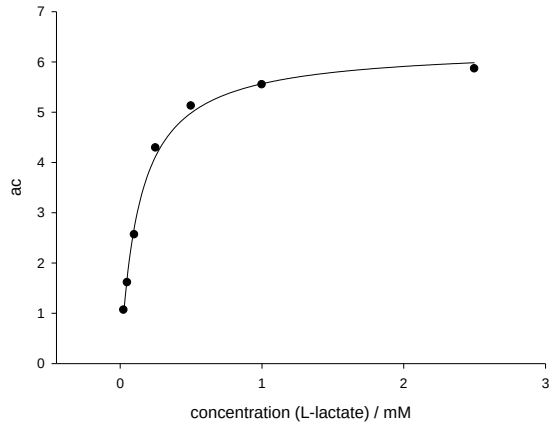

Figure Y **Y215F at pH9.0**

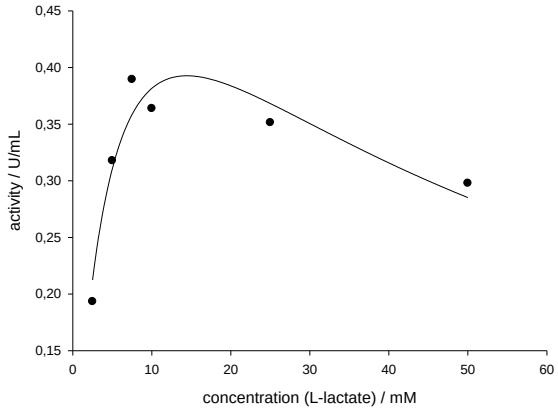

Figure Z **Y215F at pH9.5**

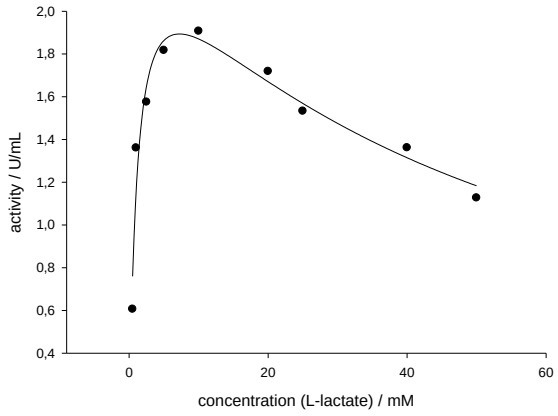

Figure AA **Y215F at pH10.0**